IAES International Journal of Robotics and Automation (IJRA)
Vol. 11, No. 2, June 2022, pp. 89∼110
ISSN: 2722-2586, DOI: 10.11591/ijra.v11i2.pp89-110

Using mobile laser scanner and imagery for urban management applications

José-Joel González-Barbosa[1], Karen Lizbeth Flores-Rodríguez[1], Francisco Javier Ornelas-Rodríguez[1], Felipe Trujillo-Romero[2], Erick Alejandro González-Barbosa[3], Juan B. Hurtado-Ramos[1]
[1]Instituto Politécnico Nacional, CICATA-Unidad Querétaro, Querétaro, México
[2]División de Ingenierías, Campus Irapuato-Salamanca, Universidad de Guanajuato, Guanajuato, México
[3]Instituto Tecnológico Superior de Irapuato (ITESI), Guanajuato, México

Article Info

Article history:

Received Aug 18, 2021
Revised Dec 24, 2021
Accepted Dec 30, 2021

Keywords:

3D point clouds
Imagery
LiDAR
Mobile data acquisition systems
Road elements segmentation
Road sign detection
Urban management application

ABSTRACT

Despite autonomous navigation is one of the most proliferate applications of three-dimensional (3D) point clouds and imagery both techniques can potentially have many other applications. This work explores urban digitization tools applied to 3D geometry to perform urban tasks. We focus exclusively on compiling scientific research that merges mobile laser scanning (MLS) and imagery from vision systems. The major contribution of this review is to show the evolution of MLS combined with imagery in urban applications. We review systems used by public and private organizations to handle urban tasks such as historic preservation, roadside assistance, road infrastructure inventory, and public space study. The work pinpoints the potential and accuracy of data acquisition systems to handled both 3D point clouds and imagery data. We highlight potential future work regarding the detection of urban environment elements and to solve urban problems. This article concludes by discussing the major constraints and struggles of current systems that use MLS combined with imagery to perform urban tasks and to solve urban tasks.

Corresponding Author:

José-Joel González-Barbosa
Instituto Politécnico Nacional, CICATA-Unidad Querétaro
Cerro Blanco 141, Colinas de Cimatario, Querétaro, C.P. 76090, México
E-mail: jgonzalezba@ipn.mx

1. INTRODUCTION

The accelerated urban growth of these days requires essential changes in what we usually know as urban construction, production, and management. In this sense, society's efforts to adapt itself and try to dominate the urban revolution comes along with a remarkable and continuous technological progress. Public and private organisms that regulate, inspect, and monitor public services have adopted technological tools for specific tasks like urban digitization tools for map building in projects related to land, road, or natural resource management. Additionally, areas such as topology, video games development, and historic preservation are in the constant search for look for better technologies, sensors, and techniques to generate the most precise digitization of urban elements.

This work explores urban digitization tools applied to three-dimensional (3D) geometry to perform urban tasks. Nowadays, mobile laser scanning (MLS) systems on board moving vehicles are one of the most common tools for data acquisition in urban environments. These on board systems combine high-range laser

sensors for 3D point cloud acquisition, panoramic cameras for image color and texture acquisition, and a global positioning system (GPS) for location tracking. MLS systems can be helpful for a wide variety of applications in areas such as archeology (e.g. land exploration), video game development (e.g. 3D object reconstruction), topology, and historic preservation. Additionally, MLS data is used to evaluate buildings (construction management, and civil engineering) and streets (urban maintenance, and electrical work). Moreover, in urban tasks, MLS data is particularly useful for projects benefiting communities (environmental projects).

Extensive research on MLS systems is easily verifiable thanks to the numerous works reported in the literature. Each of these initiatives introduces novel MLS developments from different perspectives. It is essential to compile data processing methods in photogrammetry and remote sensing and compare different scattered 3D points registration techniques [1]. Besides, Cheng *et al.* [2] made a brief review of LiDAR technologies, including terrestrial, aerial, and satellite laser scanning across multiple applications.

MLS has proven to be an excellent tool for urban management-related applications such as building facade reconstruction, road inventory, land exploration, and structural monitoring, to name a few. The researchers [3]-[6] examine different MLS applications to discuss technological advances in data registration , geo-referencing of scanned data, and environment change detection and deformation monitoring for engineering surveying and structural and civil engineering. Also, Matikainen *et al.* [7] is an exclusive review for power line corridor remote sensing methods exploring different LiDAR technologies. Many studies such as those reported in [8]-[10] report, describe, and compare urban object recognition and classification methodologies using MLS.

Some years ago, urban data acquisition systems were integrated only by laser scanner devices to replace vision systems as the primary tool for handling urban tasks. However, it did not take long for vision systems to be integrated into the solution again. Including camera vision systems into urban data acquisition systems provides texture and color data to laser scanning data. In this sense, the researchers [11], [12] examine multiple procedures for 3D reconstruction and 3D modeling from LiDAR and image integration for visualization and aesthetics. Similarly, Ma *et al*. [13] studied LiDAR-based mobile mapping and surveying technology by analyzing the performance of exceptional mobile terrestrial laser scanning systems. Additionally, the authors reviewed the positioning, scanning, and imaging devices integrated into these systems. Similarly, works such as those proposed by [14]-[16] have managed to compare mobile LiDAR technology, including system components. More recently, Wang *et al.* [17] is a review of MLS systems for urban 3D modeling where check the efficiency and stability of these systems. The main application are 3D modeling, LiDAR simultaneous localization and mapping, point cloud registration, feature and object extraction, semantic segmentation, and processing applying deep learning. In addition, Gao *et al.* [18] presents a 3D LiDAR dataset to review the size, diversity and quality, which are the critical factors in training deep models. They showed an organized survey of 3D semantic segmentation too including the latest research trend using deep learning techniques.

The combination of MLS data with imagery in vision systems helps retrieve more details of urban objects. Consequently, MLS initiatives combining imagery may be classified depending on the object to be detected, such as road markings, road signs, and pole-like objects. The works reviewed in this paper introduce MLS developments and discuss the performance and applicability of such developments to demonstrate that MLS systems are suitable for different urban management applications.

This work exclusively compiles scientific research that merges both MLS data and imagery from vision systems. A similar work is proposed by [19], who conducted a study on photogrammetry and remote sensing to point at the benefits of using both types of data for disadvantage compensation. More recently, Zhong *et al.* [20] is a survey of the MLS and camera systems fusion and enhancement. The work review both two sensors regarding depth completion, 3D object detection, segmentation and tracking. In the case of our review, the main interest is to know how current initiatives for handling urban management task successfully integrate MLS with imagery, since we found a gap regarding the use of 3D point cloud data along with imagery in urban applications.

The main contribution of this review is to trace the evolution of MLS with imagery technologies applied in urban applications. We do not review, however, autonomous vehicle MLS systems, as we consider they deserve a study of their own. We review applications that can be used by both public and private organizations in urban environments such as construction management, urban maintenance, environmental projects, electrical work, and civil engineering for management tasks such as historic preservation, roadside assistance, road infrastructure inventory, and public space study. Hence, this paper pinpoints the potential of data acquisition systems that use both 3D point clouds and imagery data to detect urban elements and solve urban problems.

We include a section to describe MLS and vision system technology to provide an overview of the tools used to accomplish such urban tasks. Namely, we focus on listing MLS developments showing data processing, segmentation, detection, and classification capabilities. Likewise, we discuss the methods commonly used to evaluate the performance of such systems as well as the accuracy of their results. Then, in the discussion section, we expose how merging MLS data with imagery from vision systems is being used most and why. Finally, as our research conclusions, we highlight opportunity areas for urban tasks in which MLS data and imagery data are exploited for both academic and industrial purposes.

2. RESEARCH METHOD

Our review discusses merely scientific research that integrates MLS data with imagery from vision systems regarding urban tasks. The selected works meet the criteria: i) Data acquisition systems with at least the following components: the MLS system, panoramic cameras, and a GPS receiver; ii) Implementation of these systems in urban applications for either public or private organizations in urban environment applications such as construction management, urban maintenance, environmental projects, electrical work, or civil engineering; iii) Works discussing the data processing process and describing the object detection or segmentation method of the data acquisition system; iv) If the work discusses a data acquisition system with object classification capabilities, then, the used classification and evaluation techniques must be described along with the accuracy of the system's results; and v) Some of the main keywords for paper selection are the next listed below: LiDAR, 3D point cloud, vision system, mobile mapping systems, mobile laser scanner systems, panoramic cameras, GPS receiver, imagery, urban application, urban management, urban environment, urban object detection, urban object segmentation, urban object classification, buildings, threes, road signs, road elements, and road markings.

Our search covers approximately ten years of research to trace the evolution of data acquisition in urban contexts. We focus exclusively on compiling scientific research that merges MLS data with imagery data from vision systems. We leave aside data acquisition developments mounted on autonomous vehicles, since we consider they deserve a study of their own. Also, we consulted the datasheets of every system reviewed. The search of works was conducted on search tools such as Google Scholar, ResearchGate, Scopus, Mendeley, and multiple journal engines. In the last ten years, there has been a remarkable increase in urban digitization developments. Figure 1 depicts the yearly distribution of works published on state-of-the-art technologies merging MLS data with vision system images in the context of urban projects. The dotted line shows clearly that there is a trend that will continue increasing. As cities around the world continue to grow exponentially, these developments will remain on the rise to help societies overcome emerging urban challenges and dominate the latest urban revolution. Figure 2 shows the principal LiDAR sensors count, some works do not specify the sensor.

Figure 1. State-of-the-art scientific article count per year that merges both MLS data and vision system images. The dotted line shows the trend line

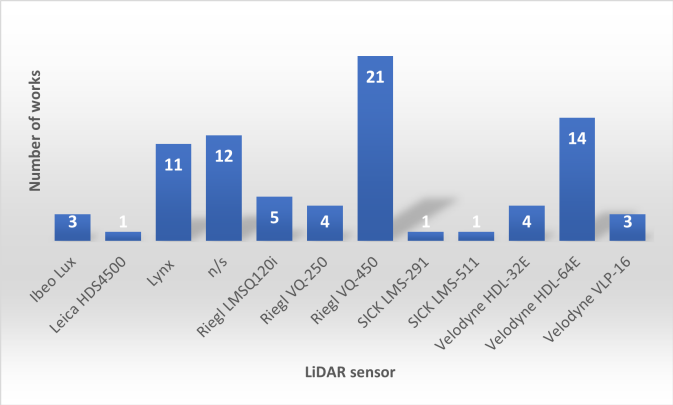

Figure 2. Principal LiDAR sensors count, some works do not specify the sensor

3. MOBILE DATA ACQUISITION SYSTEMS

The past couple of decades have witnessed the exponential growth of computational calculation and data management technologies, thus leading to rapid computational technology developments, especially in term of computer vision and computer graphics. In this sense, mobile mapping systems (MMS), especially MLS systems, have demonstrated to be effective tools in a wide range of urban applications. The satisfactory performance of MLS systems is due to their sensory system, which provides dynamic vision to any vehicle using the components: i) A laser scanner sensor: range sensor, LiDAR sensor; ii) Vision sensors: digital cameras, video cameras, and panoramic cameras; and iii) A global navigation satellite system (GNSS): GPS receiver, inertial measurement unit (IMU), odometers, speedometers, and accelerometers.

LiDAR sensors are the main element of mobile data acquisition systems referring to MLS or MMS. In turn, each MLS and MMS platform has different applications. In this work, we only review vehicle-mounted MLS systems and MMS that use both 3D point cloud and imagery for urban application scanning. As previously mentioned, we discard those platforms used for autonomous driving since we consider that these systems deserve their own study. Our goal is to describe the technologies into MLS system and vision system. Table 1 summarizes our review of vehicle-mounted MMS and MLS systems by including the information: i) Name of the system or institution that developed or integrated the system; ii) The model of laser scanner sensor; iii) The model of vision sensor including the field of view (FOV) and the resolution; iv) Model of GNSS/IMU receiver system; and v) The authors for reference. Also, we briefly describe how each system merged the MLS data with imagery data and which urban tasks was cover. Additionally, we introduce Table 2 to highlight the characteristics of the laser sensors comprised in each reviewed system, along with aspects such as data update rate, FOV, data acquisition range, and image resolution. We also consulted the datasheets of each system to obtain more details on its characteristics.

The first platform reviewed concerns the Finnish Geodetic Institute (FGI) sensei, developed at the Finnish Geodetic Institute. According to Jaakkola *et al.* [21], FGI sensei is a modular measurement system capable of performing aerial scanning and MLS mapping. The system uses an Ibeo Lux laser scanner for individual tree measurements. The researchers used FGI sensei to classify tree species by integrating laser and hyperspectral data. The camera in this system can bring RGB synchronized point cloud data and images to identifying urban objects and a mapped overview of the environment [22]. FGI sensei also uses a spectrometer that measures incoming light by passing it through a diffraction grating to a monochromatic charge-coupled device (CCD) sensor. The spectral channels were averaged for data acquisition by binning the pixels on the CCD sensor into 123 channels [22].

The second platform reviewed is VIAMETRIS MMS a vehicle for road surveying developed by [23]. The system can extract road inventory (markings and signs) by reflecting feature information from four SICK LMS-291 LiDAR sensors. In turn, camera data help texturizes and interpret this information to show the results in a geographic information system (GIS) to be consulted through internal software.

Table 1. Different MLS platforms for urban management applications

System name or insitution	Laser scanner sensor	Vision sensor Field of view FOV (H×V)	GNSS/IMU receiver systems	References
FGI Sensei	Ibeo Lux	AVT Pike F-421C 4 MP 2048 × 2048 Specim V10H 44.4° V	NovAtel SPAN-CPT Novatel 702 GG	[21], [22]
VIAMETRIS	Four SICK LMS-291	AVT Pike F-210C 2.07 MP 1920 × 1080	Trimble Omnistar 8200-H Ixsea LandINS	[23]
eXperimental Platform (XP-1)	RIEGL VQ-250	FLIR thermal SC-660 3.2 MP 640 × 480 5-CCD multispectral camera	Ixsea LandINS	[24], [25]
East China Normal University VBLS	Two SICK n/s	Two CCD cameras 1392 × 1040	GPS, INS and Odometer n/s	[26]
NAVTEQ True	Velodyne HDL-64E	Ladybug 3 1600 × 1200 HD Prosilica cameras n/s	GPS/IMU/DMI n/s	[27], [28]
National Polytechnic Institute	Velodyne HDL-64E	Point Grey Ladybug2 1024 × 768	ProMark 3 GPS CHR UM6 gyro	[29]-[31]
VISIMIND	Leica HDS4500	Six 2-4 MP SONY digital cameras	Imar GMBH GPS/GLONASS Topcon	[32]
Stereopolis II	Two RIEGL LMSQ120i Velodyne HDL-64E	Sixteen Pike full HD cameras n/s	POS-LV220	[33]
Topcon IP-S2	Three 2D SICK n/s	360° Six digital camera 1600 × 1200	GPS/GLONASS and IMU signlas tracker n/s	[34]
Topcon IP-S3 HD1	Velodyne HDL-32E	360° LadyBug 5 30 MP (5 MP × Six sensors) 2048 × 2448	GPS/GLONASS and IMU signlas tracker n/s	[35]
Optech Lynx	Two Lynx sensor	Four Lynx BB-500 GE 5 MP 57° × 47° FoV	POS LV 520 Applanix	[36]-[40]
SSW	360° laser sensor n/s	Ladybug 3 1600 × 1200	GPS receiver and IMU n/s	[41], [42]
RIEGL VMX 250	Two RIEGL VQ-250	Six VMX-250-CS6 5 1.4 MP, 2 MP or 5 MP	IMU/GNSS n/s	[43]
RIEGL VMX 450	Two RIEGL VQ-450	VMX-450-CS6 5 MP 2452 × 2056 80° × 65° FoV Ladybug5 30 MP (5 MP × Six sensors) 2048 × 2448	IMU/GNSS n/s	[42]-[49]
Trimble MX-8	Two RIEGL VQ-250	Four Point Grey Grasshopper GRAS-50S5C 5 MP 2448 × 2048	Applanix POS LV 520	[50]
Florida Atlantic University	Velodyne HDL-32E	Cameras—Nikon 3200, 3300 24.4 MP 6045 × 4003	Geodetics, Geo-iNav	[51]
Purdue University	Two Velodyne HDL-32E	5MP FLIR Flea-2G camera	Novatel SPAN-CPT	[52]
Utah Department of Transportation (UDOT)	Velodyne HDL-32E Laser road imaging system n/s	Imaging technologies n/s	Laser rut measure system n/s Position orientation sys. n/s	[53], [54]
Wuhan University	Three low-cost SICK n/s	Ladybug 3 1600 × 1200	GPS/IMU n/s	[55]
StreetMapper 30	RIEGL VQ-250 or VQ-450	DigiCAM K14 or Nikon D300 SLR 12.3 MP 4288 × 2848	NovAtel OEMV-3 or High quality IGI navigation system	[56]-[58]
Tsinghua University	Velodyne HDL-64E	Basler digital camera 1292 × 964	n/s	[59]
MODISSA	Two Velodyne HDL-64E Two Velodyne VLP-16	Eight Baumer VLG-20C.I. Jenoptik IR-TCM 640 thermal infrared camera JAI CM 200-MCL gray scale camera Jenoptik DLEM 20 laser rangefinder	Applanix POS LV V5 520 INS/GNSS DMI/IMU	[60]
AnnieWAY	Velodyne HDL-64E	Two FL2-14S3M-C and two FL2-14S3C-C Point Grey Flea 2	OXTS RT 3003	[61]
Innopolis University	Velodyne VLP-16	Basler acA 1300-200uc	NV08C MTi-G-710	[62]
KAIST Daejeon, South Korea	Two Velodyne VLP-16 Two SICK LMS-511	Two FLIR FL3-U3-20E4C-C 1280 × 560	EVK-7P U-Block GRX 2 SOKKIA MTi-300 Xsens LM13 RLS	[63]
Teledyne Optech Maverick	32-line LiDAR sensor	Ladybug 5 panoramic camera	GNSS system	[64]

*no specified (n/s)

Table 2. Different laser scanner sensors in mobile data acquisition systems

Laser scanner sensor	Company name	Data update rate Hz	Field of view FOV (HxV)	Acquisition range	Resolution points/second	Energy consumption
Ibeo Lux	Ibeo Automotive Systems GmbH	50 Hz	$110^\circ \times 3.2^\circ$	0.3 to 200 m	38,000	9 - 27 V 8 W (average), ¡ 10 W (max)
Leica HDS4500	Leica Geosystems	10 to 20 Hz	$360^\circ \times 310^\circ$	1 m to 25 m	Up to 500,000	24 V 50 - 70 W
Lynx	Optech Lidar Imaging Solutions	500 kHz	360° H	200 m max	1,000,000	12 V 30 A
RIEGL LMSQ120i	RIEGL laser measurement systems	30 kHz	80° H	Up to 150 m	10,000	24 V 2 A
RIEGL VQ-250	RIEGL laser measurement systems	300 kHz	360° H	Up to 500 m	100	18 - 32 V 180 W (max)
RIEGL VQ-450	RIEGL laser measurement systems	550 kHz	360° H	Up to 800 m	200	18 - 32 V 180 W (max)
SICK LMS-291	SICK Sensor Intelligence	75 Hz	180° H	80 m	361 (infer)	24 V 30 W
SICK LMS-511	SICK Sensor Intelligence	100 Hz	190° H	80 m	361 (infer)	24 V 22 W
Teledyne Optech Maverick	Teledyne Optech	n/s	360° H $\pm 10^\circ$ -30° V	Up to 100 m	Up to 700,000	12 V - 36 V
Velodyne HDL-64E	Velodyne LiDAR	5 to 20 Hz	$360^\circ \times 26.9^\circ$	Up to 120 m	Up to 2,200,000	12 - 32 V 60 W
Velodyne HDL-32E	Velodyne LiDAR	5 to 20 Hz	$360^\circ \times 41.33^\circ$	Up to 100 m	Up to 695,000	9 - 18 V 12 W
Velodyne VLP-16	Velodyne LiDAR	5 to 20 Hz	$360^\circ \times 30^\circ$	100 m	300,000	9 - 18 V 8 W

n/s no specified

The third system is the experimental platform (XP-1) a MMS designed and implemented by [24] at Maynooth University. The innovative 5-CCD multispectral camera in XP-1 is capable of sensing across visible and infrared bandwidths. Kumar *et al* [25]. implemented binary morphological processes and road marking generic dimension data, and eliminated extra road elements by thresholding.

The East China Normal University developed a SICK-vehicle-borne laser scanning (VBLS) [26], the fourth platform reviewed. The goal of the system was to extract street lamp distance data, and it demonstrated to be valid in terms of the accuracy of positioning and modeling ground targets. The method in the SICK/VBLS system first finds the nearest shooting position of each image record. Then, the system calculates distances between each laser point and each imaging position to discard laser points that lie beyond a distance threshold from the shooting position.

Next, Chen *et al*. [27] and Babahajiani *et al* [28] implemented the NAVTEQ True MMS for urban applications, as fifth platform reviewed. On the one hand, Chen *et al*. [27] relied on the system to focus on facade-aligned and viewpoint- aligned street-level image data to improve city scales in reconstruction. The authors employed panoramic cameras to construct a visual database of omnidirectional images and query images captured using traditional perspective cameras. On the other hand, Babahajiani *et al* [28] used NAVTEQ True technology to develop a street scene semantic recognition framework by labeling datasets. The system makes a correspondence between 3D points and combinations of 2D imagery pixels.

The sixth platform is from the National Polytechnic Institute of Mexico (IPN, by its Spanish acronym). They assembled its own MLS system for 3D urban reconstruction and conducted a sensitivity analysis of the laser sensor's calibration and the panoramic camera [29]-[31]. The accuracy in terms of texture extraction is a function of the distance between sensors. Each 3D point is projected onto the panoramic image and classified according to its distance from the camera. From a similar perspective, Garcia-Moreno *et al*. [29] developed an automated 3D city reconstruction platform for geo-referenced 3D reconstruction of outdoor scenes. According to the researchers, the system can generate global textured models while preserving the geometry of the scanned scenes by using the information of uncertainty and sensitivity evaluation, and getting a good visual appearance.

In collaboration with KTH Royal Institute of Technology, VISIMIND developed VISIMIND MMS [32], a system using imagery and laser data to obtain a geo-referenced inertial navigation system (INS), the seventh platform reviewed. In this approach, imagery and laser data help determine object position and attitude to back IMU navigation. Meanwhile the eighth platform reviewed, Stereopolis II was developed by [33] and emerged as a hybrid image/laser MMS. The system can capture a spatial data infrastructure compliant with several applications across the web, from multimedia immersive visualization to 3D metrology. Additionally, the street view application in Stereopolis II displays a pedestrian view of streets and map interaction to update precise urban maps.

As nineth and tenth platform reviewed is the IP-S2 and IP-S3 mobile survey systems from Topcon. The IP-S2 comprises a camera, a LiDAR sensor, and a GNSS system configuration. The system was created by [34] and allows for road element extraction and georeferencing by 3D to 2D re-projection of data and image processing. Likewise, the system has an automatic process forobject extraction from co-registered data. The IP-S's counterpart, IP-S3 HD1 MMS, was developed by the same company and can acquire overlapping colored images and dense point clouds. In their work, Hussnain *et al*. [35] implemented a feature detection, extraction, and matching method using the two Topcon MMSs along with aerial orthoimages.

The eleventh platform reviewed is the Lynx MMS from Optech. The Lynx can generate LiDAR and image data and has been implemented by [36]-[39]. Puente *et al*. [36] used Lynx MMS and obtained thresholds to classify eight-bit color histograms (RGB 0,0,0 zero - 255,255,255 white), whereas Riveiro *et al*. [37] managed to identify road elements by using point cloud intensity data. The method extracts road elements by thresholding intensity images. Another work, Soilan *et al*. [38] used Lynx MMS to re-project 3D synchronized road elements point cloud positions onto 2D pixels. Then, they used machine learning to identify the road elements. More recently, Safaie *et al.* [40], they developed an automated tree inventory based on Hough transform and active contours. Even though they assemble their own binary images, google images are used to compare the results. Arcos-Garcia *et al.* [39], their MMS gets traffic signs using the retro-reflective paint feature from RGB projected images. The work applies a deep artificial neural network (D-ANN) with convolutional and spatial transformer layers to extract traffic signs.

On the other hand, Capital Normal University and the Beijing Geo-Vision Technology Limited Liability Company jointly developed the vehicle-borne scanning system SSW MMS [41], [42]. The main data retrieved by this twelfth system are point clouds acquired by the laser scanner. Also camera images provide texture to implement object reconstruction and detection. Yang *et al.* [42], color and intensity features are used to create multi-scale super-voxels, while in the work of [41], 3D point clouds are the main data retrieved by the system, whereas textural information from cameras complements 3D urban environment model reconstruction.

RIEGL laser measurement systems comprise 2D and 3D laser scanners suitable for mobile mapping applications. The thirteenth and fourteenth platform reviewed are RIEGL VMX 250 and RIEGL VMX 450. Moreover, they can register scanned data acquired from moving platforms. Landa and Prochazka [43] relied on the RIEGL VMX 250 system for sign detection by reflexivity filtering. Namely, since road signs contain highly reflexive paint, the information obtained from RGB images was the color of these signs. If compared to the RIEGL VMX 250 system, RIEGL VMX 450 has been used in a larger number of applications in [42], [44]-[48]. Yang *et al.* [42], the RIEGL VMX 450 system was used to generate a multi-scale super-voxel, where point attributes such as colors, intensities, and spatial length form the super voxel. The goal is to generate a segmentation by graphics and multiple cues as main direction and colors. Wu *et al.* [44], RIEGL VMX 450 was used to develop a novel method for traffic sign detection and visibility. Said method uses the high retro-reflectivity of the traffic signs and a visibility estimation method. Yu *et al.* [45], the RIEGL VMX 450 system helped retrieve a collection of usual traffic sign pictograms and stamps from the Chinese Ministry of Transport. Then, the researchers used a Gaussian-Bernoulli deep Boltzmann machine (GDBM) to represent these signs and reduce the size of the stamps to an 80×80-px square.

Wen *et al.* [46], the RIEGL VMX 450 system was used to develop a spatial-related traffic sign management procedure. The sign area is extracted from the point clouds. Then, the 2D image data is re-projected to the point cloud data for sign recognition. From a different perspective, You *et al*. [47] introduced a traffic sign identification and fast deterioration examination method for typical environments. The approach uses a deep neural network (DNN) and Fast R-CNN.

Finally, Guan *et al*. [48] and Guan *et al*. [49] relied on RIEGL VMX 450 to propose a method for detecting traffic signs directly from mobile LiDAR point clouds based on prior knowledge on aspects such as road width, pole height, material reflectance , geometrical structure, and traffic sign size. Additionally, the system uses traffic sign image segmentation by projecting the detected traffic sign points onto the digital images. And more recently employed a convolutional capsule network model for classification.

Guan *et al*. [50] tested the performance of Trimble MX-8, a commercial MLS system that generates rich survey-grade laser and image data for urban surveying. This fifteenth system reviewed was tested at two test sites in urban areas for road network update and management tasks. As its main capabilities, Trimble MX-8 proved to be efficient in terms of extracting digital ground models, measuring tunnel height and road width, identifying traffic signs, reconstructing 3D building models, monitoring land-side, and configuring utility.

Next are the sixteenth and seventeenth platform checked, in [51] and [52], the Velodyne-HDL32E

system was used to improve the accuracy of point clouds and imagery recordings. The eighteenth platform is in [54]. The work discussed a mobile-based data collection approach developed by the Utah Department of Transportation (UDOT). The systems developed comprise a laser scanner, an imaging sensor, a distance and crack measurement module, and other methods. The goal of the UDOT approach is to get high-resolution road sign images. First, daytime digital photos of road signs were captured. Then, trained operators examined such photos to rate the visual condition of the signs as good, fair, or low (GFP). From a different perspective, in collaboration with Wuhan LEADOR Spatial Information Technology Co., Wuhan University developed its own MMS. Cui *et al.* [55], this nineteenth system is used to propose a line-based registration approach for panoramic images and LiDAR point clouds. The researchers established the transformation model between the primitives from the two datasets in the camera-centered coordinate system. Also, using extracted features, they resolved the relative orientations and translations between the camera and the LiDAR.

The twentieth platform is the StreetMapper 360 MMS and is mainly used for road mapping and urban environment reconstruction. Yadav and Chousalkar [56], this MMS is a part of a power line extraction method. The acquired point cloud is first organized as 2D gridded data, which take the shape of connecting pillars in 3D. The 2D Hough transform was used on the image data to detect power lines as linear features. On the other hand, Yadav *et al.* [57], StreetMapper 360 MMS is used within a method for calculating road geometry parameters (i.e. width, centerline, longitudinal, and cross slope). Onsite manual measurement reference data were used to verify the correct functionality of the method. The data included road slopes diagrams using MLS data (XYZRGB format) of road surface points.

The twenty-first platform is in [59], researchers from Tsinghua University handled a Velodyne HDL-64E system with a Basler digital camera (1292×964 resolution) to acquire both color and geometrical data. Planar objects are directly detected in 3D space from colorized laser scans containing both color and geometrical data. The authors applied a driving cuboid aligned along roadway boundaries, and the laser scans falling into the camera FOV can collect color data.

The Fraunhofer Institute of Optronics developed the sensor vehicle MODISSA. The twenty-second platform reviewed allowed the development and testing of real time methods or high level driver assistance functions. The functionalities were applied in LiDAR-camera pedestrian detection methods [60]. Zhu *et al.* [65] used MODISSA to generate a unified thermal point cloud without the need for RGB images. The fusion helps to describes the radiance of building facade and to analyze thermal properties.

The Karlsruhe Institute of Technology and the Toyota Technological Institute at Chicago (TTIC) developed the AnnieWAY MLS system and used this twenty-third platform reviewed to develop a novel set of computer vision benchmarks, known as the KITTI vision benchmark. The task to accomplish and improve with the KITTI suite include stereo, optical flow, visual odometry, 3D object detection, and 3D tracking. Bruno *et al.* [61] applied the KITTI benchmark suite to their 3D traffic sign detection method to track traffic sign objects and their images. The method can identify traffic signs by integrating 2D and 3D data and building a semantic object interpretation.

Velodyne's VLP-16 sensor is the smallest advanced sensor in Velodyne's 3D LiDAR product range. Buyval *et al.* [62] proposed a method on board an autonomous vehicle for road sign detection and localization using the VLP-16 sensor. The researchers used this twenty-fourth platform reviewed to implement their algorithm for road sign s classification and localization in a 3D space. The algorithm uses neural networks and points clouds obtained from a laser range finder. From a different perspective, Korea Advanced Institute of Science and Technology (KAIST) developed its own MMS. Jeong *et al.* [63] incorporate stereo camera data into KAIST MMS, the twenty-fifth platform reviewed to support vision based robotics research. As its main contribution, this approach provides data for a variety of environments, from downtown area to apartment complexes to underground parking lots. Also, the approach provides a baseline via a SLAM algorithm using highly accurate navigational sensors and a semi-automatic loop closure process.

The Toronto-3D data set was acquired through the Teledyne Optech Maverick Weikai [64], the twenty-sixth platform reviewed. The dataset covers approximately 1 km of point clouds and consists of about 78.3 million points. The inspiration for the data set was semantic segmentation to train deep learning models effectively. The data set is about 8 urban object categories as road, road marking, natural, building, utility line, pole, car, and fence.

According to this review, RIEGL VMX-450, Optech Lynx Mobile Mapper, and Velodyne HDL-64 are the most popular MLS tools applied in urban tasks. RIEGL VMX-450 is a robust integrated system with its own sensors; Optech Lynx Mobile Mapper, however, is less robust than RIEGL but includes both digital

cameras and GPS receivers. In turn, the Velodyne HDL-64 laser scanner sensor is robust but only comprises a laser scanner sensor. In conclusion, the choice of a given MLS system over others may largely depend on multiple factors (e.g. costs), yet integrated MLS systems are more appropriate. Also, MLS systems integrate GPS receivers and cameras, which grant simultaneous registration of visual and spatial data. Nevertheless, it is essential to maintain a cost-balance benefit. It is well known that one of the most common problems in the use of MLS systems concerns the existence of large occluded regions and segmentation. A not so expensive solution to this problem is to retrieve multiple scanned images of the same area; however, developments of segmentation methods are by themselves case studies.

4. URBAN MANAGEMENT APPLICATIONS

This section discusses the evolution of MLS technology combined with imagery for urban applications. We list those systems using data processing, segmentation, detection, and classification methods. We also discuss the accuracy of the results provided by these systems and the evaluation methods used to assess their performance. Objects in urban environments include buildings, pedestrians, vehicles, road signs, trees, and animals, among others. Dynamic objects (e.g. vehicles, pedestrians, animals) are studied mainly for obstacle avoidance by autonomous vehicles or to analyze the flow of objects in physical space. On the other hand, static objects (e.g. trees, road signs, traffic lights, lamps, buildings, streets, and services) are studied to ensure their good condition and location and trace their change over time due to weather conditions or vandalism. Also, static object features serve multiple different purposes (e.g. safe transit, environment preservation, historic preservation, public space study, archaeological or architectural analyses).

The initiatives reviewed in this section are systematically organized in four tables. Each table includes the following information: i) author names, ii) acquisition system, refer to the section 3, iii) urban object classes detected, iv) data processing methods, 3D point clouds, and imagery enhancing or reduction, v) detection and segmentation, methods implemented, vi) classification methods used, and vii) accuracy, performance, and results obtained. Table 3 summarizes our review of works dealing with mixed (i.e. dynamic and static) object detection. Then, Table 4 lists the reviewed developments on static objects (i.e. trees, road signs, traffic lights, lamps, buildings, streets, and services). Notice that studies on road signs are listed in a separate Table 5, due to the large number of scientific developments revolving around road sign detection and visualization. Finally, developments dealing with road elements (e.g. road markings, crosswalks, lanes, arrow signs, sidewalks) are summarized in Table 6. The following sections provide a thorough discussion of each Table.

4.1. Urban management applications from mixed dynamic and static urban objects

Table 3 introduces a compilation of works on static and dynamic urban object detection and classification. Detection of mixed urban objects is applied in scene analysis, roadside assistance, or obstacle avoidance, being vehicles, people, and urban elements such as trees the most commonly detected. Urban objects detection efficiently supports urban surveying, geospatial data acquisition by GPS, and safety assessment in pedestrian crossing environments. There is a scientific proof that mobile mapping is a reasonable means for analyzing specific safety parameters in urban environments. The first step in data processing is plane extraction. Segmentation of ground and facade points reduces the amount of information to be analyzed and facilitates problem-solving. As researchers [66]-[69] pointed out, methods such as the random sample consensus (RANSAC) and the M-estimator sample consensus (MSAC) are popular because their implementation is more accessible than other methods, such as gridding and voxelization. These two last techniques group 3D points into perceptually meaningful clusters with high efficiency. Also, supervoxelization allows for clustering spatially connective points within similar features [66], [42], [67], [68]. Supervoxelization is often preferred over other segmentation methods because of its basic processing units instead of original points in point cloud applications. Object detection and segmentation depend on the classes to be identified. If the goal is building and road reconstruction, data processing achieves object segmentation. For other objects, such as dynamic and static urban objects, vectors are usually favored. Feature vectors include geometry features (dimensions, color, and intensity), [28], [70], [66], [71]-[73], [69]. The connected component algorithm is usually used for segmentation, since it operates on organized point cloud data, [71], [74], [75], [69]. Also, the algorithm is based on the costly neighborhood and uses normal surface points in Euclidean space, commonly used in point clouds. Points are compared using a comparison function to determine the neighborhood of the point cloud. Since most works using urban objects are to discern among classifications, the classification process only needs to find general classes. In this sense, the main classifier methods include super vector machine (SVM), [74],

[71], [70], fuzzy logic [66], boosted decision trees [28], [67], [68], and convolutional neural networks (CNN), [75], [73], and [69]. All these methods consider machine learning techniques, whose objective is to learn by acquiring knowledge by training a given data set. Accuracy validation methods include the confusion matrix and the F-score [66], [75], [72]. The F1-score is the harmonic mean of the precision and recall, where an F1-score reaches its best value at 1 (perfect precision and recall) and its worst value at 0. Results have shown that accuracy decreases as more object details are to be detected. Serna and Marcotegui [74] studied eight object classes: cars, pedestrians, noisy structures, dogs, house facades, chimneys, trees, and lampposts. The detection method segmented 78% of the objects accurately, and 82% of such well-segmented objects were correctly classified using SVM and connected components. Babahajiani *et al.* [68] proposed a method that can classify eight different classes of urban objects – buildings, trees, cars, traffic signs, pedestrians, roads, water, and sky using a boosted decision tree detector. The method had a classification accuracy ranging from 83% to 67%. Also, Luo *et al*. [73] used three data sets with nine, six, and 14 classes, respectively. They implemented a CNN with feature vectors of the objects. The lowest accuracy result (74.9%) was obtained in the 14 object data set.

Table 3. Urban management applications from mixed dynamic and static urban objects

Reference	Acquisition System	Classes	Data Processing	Detection and Segmentation	Classification	Accuracy
[28]	NAVTEQ True	Sky, Building, Road, Tree, Car, Sidewalk, Sign-S, Fence, Pedestrian and Water	3D-2D projection between patches and super pixels SPs	3D features: height above camera, surface planarity and reflectance strength	Boosted decision trees, each 3D feature vector with a semantic label	88%
[70]	Stereopolis II	3D buildings, 3D roads and a set of 3D visual landmarks	not specified	Bottom-up algorithm given the objects geometric specifications	Rigid stereo pairs are used for 3D recognition and modeling	qualitative
[66]	Velodyne HDL-64E, a monocular camera and other sensors	Ground (road), building, water, tree, grass, bush, pavement, sky and obstacles (vehicles, pedestrian)	Separate the ground points using a RANSAC plane fitting algorithm and candidate obstacles are localized into 3D cubic voxel grid	Bottom-up classification of local image patches and top-down contextual analysis to further resolve uncertainties	Fusing result of Velodyne data and image using the fuzzy logic inference framework, and smooth result by the Markov random field based temporal fusion method	F-measure MRF: 0.25-0.59, MFV 0.24-0.53
[74]	Stereopolis II	Car, pedestrian, noisy structure, dog, house facade, chimney, trees, and lampposts	3D point cloud projected to elevation images, segmented facades as the highest vertical structures and eliminated small and isolated regions	Connected objects are segmented using a watershed approach	SVM with geometrical and contextual features	det. = 98% seg. = 78% class. = 82%
[42]	RIEGL VMX-450 and SSW	Buildings, streetlamps, trees, telegraph poles, traffic signs, cars	Hough transform to filter the facade and Top-Hat for hole filling on the ground	Multi-scale supervoxels using the point attributes (colors, intensities)	Semantic knowledge	91%
[71]	FGI Sensei	Trees, lamp posts, traffic signs, cars, pedestrians, and hoardings	PCA and connect components to remove ground and buildings	Local descriptor images (LDH), spin images, and general features	SVM and its C-SVM version with the radial basis function (RBF) kernel	87.9%
[67]	NAVTEQ True and Stereopolis II	Tree, car, sign, person, fence, ground and building	Ground and building segmentation by RANSAC, maximal height filter and morphological operations	Voxel based segmentation and 3D feature extraction (intesity, areas and normal angle)	Boosted decision tree	91%
[68]	NAVTEQ True, and Velodyne HDL32	Building, tree, car, traffic sign, pedestrian, road, water, and sky	rule-based detectors for road surfaces and building facades, RANSAC	Super-voxel features, surface orientation by PCA, and 2D semantic segmentation	Boosted decision tree detector	83% and 67%
[75]	Velodyne HDL-64	Vehicles, pedestrians, short facades and street clutter	2D grid based approach via point height information: ground, low foreground, high foreground, and sparse areas	Fast connected component analysis for object separation, maximal elevation value and point cloud density	Theano: CNN-based feature learning framework	89% overall F-rate
[72]	Optech Lynx	Traffic light (Type 1), traffic light (Type 2), street lamp, tree, and other pole-like objects	Pedestrian crossings extraction by intensity data, vertical mean and variance computation and a region growing algorithm for ground and non-ground elements	Pole-like object segmentation by euclidean clustering and a geometric supervised classification	PCA to projected points into a 2D raster grid binary image, type 1: classification by a Cubic SVM, Type 2: a two layer feed forward neural network with sigmoid hidden and softmax output neurons	F-score 95%
[73]	RIEGL VMX-450	HDRObject9, SMDObject6, SUObject14 including bus station, light-pole, road sign, station sign, traffic light, traffic sign, trashcan, trees, vehicles, pedestrian, etc.	not specified	Three discriminative low-level 3D shape descriptors for obtaining multi-view 2D representation of 3D point clouds	JointNet, by jointing low-level features and CNNs for 3D object recognition	recognition: 94.6%, 93.1% and 74.9%
[69]	Optech Lynx	Bench, car, lamppost, motorbike, pedestrian, traffic light, traffic sign, tree, waste-container, wastebasket	Planes elimination, MSAC	Connect component	Shape and colour to CNN object classification	99.5%

4.2. Urban management applications from mixed static urban objects

Table 4 introduces a compilation of works dealing with static urban object detection and classification. Static urban object detection supports multiple purposes, such as hazard management, city planning, travel guidance, 3D reconstruction for exploration systems, and geographical information system (GIS) development. In turn, GISs allows for spatial data analysis, automatic change detection registration, geo-database updating in urban environments, and smart city management.

Table 4. Urban management applications from mixed static urban objects

Reference	Acquisition System	Classes	Data Processing	Detection and Segmentation	Classification	Accuracy
[23]	VIAMETRIS MMS	Road boundaries, road markings and traffic signs	RANSAC to extract road boarders and centers	3D NURBS for road curvature, road signs extraction by threshold on reflectivity value	qualitative	qualitative
[84]	LiDAR system and ground mobile truck data (no specified)	Tree	Point cloud filtered by the second order derivatives	Watershed transformation	Point-features-based matching algorithm in stereo vision, Föstner operator	comparison 80%-90% integrated 75%-95%
[21]	FGI Sensei	Pole-like object and trees	No specified	Clustering the extracted vertical line segments and analysis of the spatial distribution	Cluster distribution inspection vertically splited of a tree	comp. 90% correc. 86%
[26]	SICK-VBLS	Lamps	Density of Projected Points (DoPP)	Maximum height of each grid cell	Height threshold	qualitative
[22]	FGI Sensei	Tree	No specified	Hyperspectral imagery and laser overlapping information, height distributions	SVM	two species 95.8% three species 83.5%
[27]	Velodyne HDL-64E and Ladybug	Buildings	Visibility mask for spherical projection, panorama overlapping perspective central images PCIs, perspective frontal image PFI, and histogram equalization	Upright feature keypoints	Query image vocabulary tree trained on SIFT descriptors, and geometric verification for PCIs (RANSAC with a 2D affine model) and PFI (3 degree-of-freedom (DOF) scale and offset check)	recall=95%
[32]	VISIMIND MMS	Buildings facades	GPS and IMU data is integrated in post processing module (PPM) within the Kalman filter	Feature extraction based on Harris operator, and use of Lucas Kanade Feature Tracker	28 control points measured total station with accuracy of 5 mm	RMS value 0.011 m
[78]	Optech Lynx Mobile Mapper	Trees and buildings	Divides the mobile lidar points into grids on the XOY	Weights of points, georeferenced feature image and feature extraction image segmentation	Shape constraint and Z-direction profile analysis	Trees profile 97.9% Building shape 100%
[41]	SSW	Trees	Sloping adaptive neighborhood to removing the ground	Binary connected component labeling density based and crown segmentation of overlapping objects	Entity hierarchical extraction by height of the target	qualitative (10 cm error)
[36]	Optech Lynx Mobile Mapper	Luminaries	Point cloud presegmentation based on height values	Colored point cloud filtered by geometric and radiometric features	Thresholds are extracted from the color histogram analysis RGB	100% in 95s
[76]	RIEGL VMX 250	Parking railing, boards, light pole, house segment, hedge, fence, fire hydrant, warning tape, crane, chair, and bucket	Point cloud images coregistration, terrestrial images free-network bundle adjustment, control points manually collected from feature points and block window patches as a basic z-buffer unit to filter	2D Delaunay triangulation performed on the discrete points, multi-stereo image inter-correlation, and graph cut area based on the superpixel optimization	Evaluation of detection	detec. 64%, 76.4%, 80%
[43]	RIEGL VMX 250	Traffic signs, road markings and general pole-shaped objects (e.g. city lights or trees)	Reflexivity filtering	Euclidian cluster extraction	Segments processing by rules, point number, centroid and height	93%
[83]	RIEGL VMX-450	Tree	Voxel-based upward-growing filtering	Euclidean distance clustering and voxel-based normalized cut segmentation	Waveform representation, two layers deep Boltzmann machines DBMs and SVM	86.1%
[56]	StreetMapper 360	Power lines	2D gridding and horizontal segmentation based filtering of horizontal segment	2D point density based refinement to remove trees and building, Hough transform detection	Quantitative accuracy assessment	correctness 98.84% complet. 90.84%
[77]	Velodyne HDL-32E	Building and road marking	Elimination of reflected parts of sidewalks or nearby vehicles through binarization	2D probabilistic occupancy grid map for vertical structures, line extraction using Hough transform and the IEPF algorithm	qualitative, RMS position errors for the lateral and longitudinal directions	RMS: 0.136 m lateral and 0.223 m longitudinal
[79]	LiDAR sensor no specified and 360° camera	Doors and windows	Cube mapping of spherical panorama images	Pixel-wise mask and semantic segmentation on point clouds through DBSCAN and connect components	No classification	Visual evaluation 1 to 2 cm
[100]	Optech Lynx Mobile Mapper	Road vegetation	Limit the edge of the road, increased point density	Polygonal region segmentation within 10 m threshold	MSAC	Mean geometric error 0.25 m 2.82%
[80]	TOPCON MLS and a Ladybug-5 camera	Building facades	Ground filtering, edge center and window detection	Geometric Filtering	Kalman filtering	RMS X 0.131 RMS Y 0.135
[81]	road-borne MLS system n/s and a Ladybug 5 camera	Fences	Images cropped	FCN predictions, image to point cloud transfer using perspective projection, and polygonal segmentation using Hough transform	PointNet	Precision 95% Recall 87% K 0.89
[82]	RIEGL VMX-450	Building patches	Constraining the area of keypoint throughthe location within a 50 m radius from the image GPS position	Siam2D3D-Net: STN module and modified VGG network, to learn the image feature, point cloud branch with PointNet	No classification	Qualitative
[40]	Optech Lynx	Trees	Left-side and a right-side point cloud division, low-height points filtered	Foliage extraction by Voronoi tessellation and active contour	Characteristics measurements trunk and foliage height and diameter	Average error in height extraction: less than 15 cm, TDBH average error: less than 10 cm
[65]	MODISSA	Buildings	Intrinsic calibration of TIR images. Take of horizontal lowest plane and CC for the point clouds	Harris corner detector and the line segment detector (LSD), Harris 3D	Find correspondences and 2D/3D registration by an automatic method based on restricted RANSAC	false alarm rate = miss detected lines over detected lines less than 30% after 5 pixels

*n/s no specified

Developments extracting static urban objects process the data depending on the classes to be detected. For other urban object detection procedures, first, it is necessary to identify the ground and building points. Qin and Gruen [76], relied on a Z-buffer unit to filter points to segment three classes of static urban objects: parking railing, boards, and light poles. The authors used 2D Delaunay triangulation and supervoxelization for object detection. From a similar perspective, the works of [23], [77] used reflectivity values of road markings and traffic signs to segment and filter buildings. Both building extraction and monument extraction are highly useful in cultural heritage documentation, reverse engineering, and 3D objects reconstruction. Also, they help generate digital elevation models (DEM). Prior to object detection and segmentation, Chen *et al*. [27] and Gajdamowicz *et al*. [32] performed a data integration process to allow for more detail in point clouds. Integrating point clouds with imagery allows using 2D methods such as SIFT descriptors and the Harris Corners Detector. Yang *et al.* [78] focused on the task of building reconstruction by relying on tree detection and extraction to solve the occlusion problem. In this sense, MLS systems are possibly the best systems for detecting changes in objects eluding contact. Building detection can also deploy urban flood disaster and risk management plans [79]. Also, Ergun *et al.* [80] developed a building facade survey through a 2D Kalman filtering algorithm and a related laser data segmentation method. The method allows the acquisition of rectified images from the facade to CAD. Another work related is the work of [81]. It presents an image-based point cloud segmentation (IBPCS) method for filter the point clouds after semantic segmentation of images. They use the method in low dense point clouds as fence recognition. The detection and classification process was made using a fully convolutional network (FCN) and PointNet. Termal infrared (TI) images are used in [65] to evaluate the energy consumption and leakage of building. They fusion thermal infrared image sequences and the point clouds. The fusion describes the radiance of the facade in the building and helps to analyze thermal properties. For augmented reality, Liu *et al.* [82] used 2D image patches and 3D LiDAR point cloud from the urban scene. They proposed Siam2D3D-Net to achieve virtual-real registration high-quality using 2D-3D patch-volume dataset and retrieving the Euclidean space.

According the researchers [21], [41], [83], classification of tree species is mainly performed for safety studies, noise modeling, and environmental and ecological analyses. Trees play a critical role in urban ecosystems since they help maintain the environmental quality and aesthetic beauty of urban landscapes. Moreover, trees are of social service for communities. Tree classification relies on tree height characteristics and demonstrates that biomass changes can be mapped with relative facility using laser collections of the same tree. Gong *et al*. [84] collected tree data such as counting and dimensions for effective tree management and quantitative tree analysis in urban areas. Likewise, Zhong *et al*. [22] introduced hyperspectral sensors to classify tree species, mainly coniferous and deciduous trees. The first step in tree detection using MLS systems and imagery data is ground point filtering, followed by shape detection considering pole-like object, height, and crown density. Safaie *et al.* [40] they created a tree inventory from an MMS point cloud. They start extracting the trunk by the Hough transform (HT) followed by the tree foliage via Voronoi tessellation (VT). Then, a density image is created using the number of points as the gray value of each pixel.

Detecting urban objects such as street lamps, traffic signs, street light poles, and power lines starts by detecting pole-like objects, as in tree detection. The researchers [26], [36], [43], [56], the authors based their urban object detection approaches on point cloud density, height filter, and geometric and radiometric features. An RGB spectrum is a helpful tool for object differentiation using a color filter and threshold color histograms.

4.3. Road sign detection and classification

Table 5 lists relevant works that deal with or propose methods for traffic sign detection and classification. Traffic signs worldwide share standard features but also respond to local classifications. All strictly static urban objects have particular physical characteristics for safety and do not obstruct other activities. Namely, traffic signs have specific standards to be easily and quickly identified by drivers and pedestrians. Their spatial characteristics allow us to differentiate elevated traffic signs from lower traffic signs; geometric shapes make it easy to know whether a given sign is informative, restrictive, or preventive. Also, visual features, such as color and texture allow us to know the message being transmitted. Moreover, road signs are coated with reflective paint; hence, they reflect back the light from car headlights in order to improve readability. This feature is advantageous when using laser sensors for road sign detection and classification, since sensor-based systems can retrieve color intensity data.

Table 5. Road sign detection and classification

Reference	Acquisition System	Data Processing	Detection and Segmentation	Classification	Accuracy
[101]	Velodyne LiDAR sensor system and associated photolog	Many sign attributes, such as location, size (length and width), mount height, collection date, and facing direction were measured	color, sheeting type, age, and geographic conditions, in order to predict their retroreflective degradation over time	Visual nighttime inspection, and Retro reflectivity measurement	conditional probability, qualitative
[44]	RIEGL VMX-450	Surface extraction from point clouds by reflectance and geometric characteristic	Geo-referenced relations according to the normal of ground and four image features: intensity, color histogram, edge contrast, and proportion of traffic sign	Evaluation of the visibility level based on a combination of visual appearance and spatial-related features	Average deviation under 5%
[37]	Optech Lynx Mobile Mapper	Horizontal intensity images, thresholding and evaluation of histograms with GMM	DBSCAN and subsequent curvature analysis with PCA	Shape descriptors, 3-D points intensity image	completeness 92.11% correctness 93.96%
[38]	Optech Lynx Mobile Mapper	GMM with two components non-reflective and reflective points	DBSCAN PCA	Geometric parameters: centroid, height, etc; and color: (HLS) bitmap using HOG and SVM	98%
[46]	RIEGL VMX-450	Highly retro-reflective vertical plane	Centroid coordinates of the bottom ring, a horizontal profile with a thickness size	SVM classifier trained by a mix feature of HOG and color descriptor	detection MLS 91.63% images 92.61% precis. 96.32%
[45]	RIEGL VMX-450	Voxel cloud connectivity segmentation (VCCS)	Bag-of-visual-phrases representations	Gaussian-Bernoulli deep Boltzmann machine-based hierarchical classifier	97.54%
[39]	Optech Lynx Mobile Mapper	K- Nearest-Neighbor algorithm is used to obtain the closest voxel	Geometric and radiometric features, 3D data projected on 2D RGB images	D-ANN, convolutional and spatial transformer layers	99.71%
[47]	RIEGL VMX-450	No specified	Fast R-CNN training for detection and coarse corresponding relationship between the image and the point clouds	Traffic sign damage inspection: tilted pole, deformed board, fallen board or pole and disappeared	detec. = 92.42%
[59]	Velodyne HDL-64E S2 and Basler digital camera	Driving cuboid aligned along roadway boundaries and colorized laser scans	Laser reflectivity and RGB, HSV, and CIE $L \times a \times b$ color spaces, SVM	3D geometric characteristics of planar objects HOG	detection 95.87% recognition 95.07%
[61]	AnnieWay (KITTI database)	K-means and background subtraction	Neural Network with binary output board detection, "object signature", the 3D-CSD (3D-Contour Sample Distances) descriptor	Deep Learning CNN to classify type: maximum speed, stop, preferential, pedestrian or other	classi. = 97.64% detec.= 76%
[48]	RIEGL VMX-450, four CCD cameras, a set of Applanix POS LV 520	knowledge of pole height and road width to remove points	detect traffic sign interest regions based on intensity information and geometrical structures	on digital images, supervised GB-DBM	detection 86.8% classification 93.3%
[54]	Velodyne LiDAR sensor system and associated photolog	No specified	Sign location, size, color, condition	Random Forests model and Odds ratio	qualitative sign inspection by contingency tables
[62]	Velodyne VLP-16	Depth filtration	Bounding box and sign location on an image to find a corresponding to the sign point cloud	Faster-RCNN architecture	from 30% to 96%
[86]	RIEGL VMX-450	Objects on both sides of the lane based on the trajectory data and in a distance d are retained	Semantic and spatial properties (location, position and geometric features)	Deep neural network: YOLOv3 and FCN model	mx-pres. 95.8% mx-recll 99.25% mx-f1-m 95.77% mx-qual 91.89%
[102]	RIEGL VMX-450	Quantitative representation of the visibility and recognizability of traffic signs within Sight Distance (SD)	Visual recognizability field and Traffic Sign Visual Recognizability Evaluation Model (TSVREM)	Parameter Sensitivity Analysis	occlusion rate: 95% verification 94.89%
[87]	RIEGL VMX-450	No specified	Pole height, road width, intensity, geometrical structure, and plate size from LiDAR data	Points are projected onto the images to apply a Convolutional Capsule Network	recognition rate 0.957, detec. 86.8%
[88]	RIEGL VMX-450	A curb-based filtering method to divide mobile LiDAR data into ground and off-ground points	Euclidean clustering algorithm to extract pole-like objects and retro-reflectance properties	Convolutional Capsule Network	recognition rate 0.965, detec. 86.8%
[85]	AnnieWay (KITTI database)	Ground and building filtering regarding the driver trajectory	Object segmentation through 3D point cloud density and retro-reflective material feature. Color segmentation using HSV model	Classification through geometric shape association, local features description for semantic data	precision 0.88,
[49]	RIEGL VMX-450	Curb-based filtering method,	Euclidean clustering algorithm to extract pole-like object, next retro-reflectance properties to extract traffic signs, and Image re-projection	Deep Learning: convolutional capsule network	Recognition: 0.965

For traffic sign detection, developments take advantage of the highly retro-reflective property of the vertical plane. After ground point segmentation, laser points intensity values help segment traffic signs from other objects. Researchers [37], [38] used a Gaussian mixture model (GMM) and a density-based-approach (DBSCAN) to filter traffic signs. The GMM is a probabilistic model that can be thought of as generalizing k-means clustering to incorporate information on the covariance structure of the data and the centers of the Gaussian distributions. Traffic sign classification depends on the number of details or characteristics to be identified in the signs. Works such as those proposed by researchers [38], [46], [59] relied on the histogram of oriented gradients (HOG) to classify road signs. HOG is a feature descriptor using the gradient distribution directions. Gradients of an image are useful because the gradient magnitude is large around edges and corners. Researchers [38], [46], [59], used SVM to classify the HOG. Machine learning simplifies the traffic sign classification task by using ground truth. Tan *et al*. [45] and Yang *et al*. [48] used a GDBM-based hierarchical classifier. The GDBM uses Gaussian units in the visible layer of the deep Boltzmann machine (DBM); however, DBM is an ANN model where each neuron in the intermediate layers receives both top-down and bottom-up signals, thus facilitating uncertainty propagation during the inference procedure. Yang *et al*. [85] used the KITTI database to road signs segmentation. The object segmentation is divided in 3D point cloud and image segmentation. The first is by 3D point cloud density and retro-reflective material feature. The color segmentation is using HSV model. The preliminary classification is through geometric shape association, local features extraction and description for semantic data as numbers, characters, and drawings.

In this sense, semantic detection has simplified the traffic sign detection task. 3D information is re-projected onto 2D images, and D-ANNs are used for sign classification, as discussed in [47], [39], [61], [62], [86]-[88]. These systems use CNNs hierarchically organized based on supervised learning and contain several specialized hidden layers. This organization allows the first layers to detect lines and curves and specialize until they reach deeper layers that recognize complex shapes, such as faces or an animal silhouettes. Guan *et al.* [49] developed an automatic traffic sign detection and recognition method. They employed an euclidean clustering to extract pole-like objects and the retro-reflectance properties for traffic signs. Classification was made using a convolutional capsule network.

Table 6. Road element detection and classification

Reference	Acquisition System	Classes	Data Processing	Detection and Segmentation	Classification	Accuracy
[34]	IP-S2 HD	Lanes, arrows sign and crosswalks	Point cloud geographical re-projection, geometric filtering, interpolation on a regular grid (raster 2D image)	Labeling object isolation and morphological indicator, peak detector for lane detection, and attributes generation	Template matching for arrow marks, and crosswalks detection by morphological indicators	qualitative
[92]	RIEGL VMX-450	Longitudinal markings, transverse markings, object markings, and special markings	Vehicle trajectory raw data partitioned, and small height pseudo scan-lines for jumps detection in road curbs	Geo-referenced intensity image via an extended inverse-distance-weighted, and local and global intensity data	Image segmentation by a point-density-dependent multi threshold method to recognize road markings	complet. 0.96, correct. 0.83, F-measure 0.89
[96]	RIEGL VMX-450	Road manhole and sewer well covers	Rasterization of road surface points into a 2-D georeferenced intensity image improving the inverse distance weighted	Marked point of disks and rectangles to model the locations of manhole and sewer well covers and their geometric dimensions	Reversible jump Markov chain Monte Carlo algorithm, simulation of the posterior distribution using a Bayesian paradigm	complet. (95.16%),correct. (97.25%), and quality (92.67%)
[25]	eXperimental Platform (XP-1)	Continuous line, broken line, words, zig-zag, hatch, and arrow	Range dependent thresholding to the intensity values, and range attributes convert into 2D raster surfaces	Binary morphological operations and priori knowledge of the dimensions	Comparative analysis by the length and average width of the final extracted road markings	detec. 90.91% and 88.43%
[93]	RIEGL VMX-450	Road markings	Partition the point cloud into blocks along the trajectory, a profile is generated perpendicularly, curb points are located within each profile	Multi-segment thresholding strategy using the Otsu's, Euclidean distance clustering, voxel-based normalized cut segmentation	Large-size marks based on trajectory and curb-lines; deep learning-based small-size marks; and PCA rectangular-shaped marking classification	complet. 0.93, correct. 0.92, F-measure 0.93
[97]	Stereopolis II	Road markings	Orthophoto-like LiDAR image generation by vertically projected point cloud onto a horizontal plane (intensity and height)	Reversible-Jump Markov Chain Monte Carlo (RJMCMC) sampler coupled to detect occurrences of road marking	Local bundle adjustment (LBA), and uncertainty propagation applied to estimate pose parameters and covariance	Maximum error 0.4m
[51]	Velodyne-HDL32E	Sidewalk, median, guard rail, fencing, lighting, landscape areas, delineators, lanes, road Markings, and road signs/boards	Road centerline and road width are extracted from the TIGER (Topologically Integrated Geographic Encoding and Referencing) dataset	RANSAC to ground points, poles and lamp posts; road marking and road signs by edges from the images, and point cloud intensity; building by planar property	Attributes: dimensions, curbs, condition, geometry, message, and type	qualitative
[35]	IP-S3 HD1	Road markings	Point cloud data tiles cropped, 3D point grey values calculation of the corresponding pixels in raster image, and nadir aerial ortho image projection	Harris corner detector, adaptive approach for dynamic threshold computation, and Learned Arrangements of Three Patch Codes (LATCH)	k-NN based descriptor matching and Homography (computed with RANSAC)	qualitative by evaluation of the matching result
[90]	Optech Lynx Mobile Mapper	Pedestrian crossings and arrows	Curb pavement segmentation by k-means and intensity filter within GMM	Raster image creation and road markings detect by Otsu binarization and CC	Set of binary image features: GBF	F-scores extrac.=94% classif. 96%
[91]	Optech Lynx Mobile Mapper	Sidewalk, pavement, and road markings	Intensity values normalization, saliency analysis to segment z-axis point clouds and k-means, height filter within a 2D raster image	Ground extraction via region growing, road curb extraction by ground limits, and fusing heuristic and supervised learning methods	Reflective materials, standard deviation filter on the pavement intensity image in a 3-by-3 pixel neighborhood	F-score detec. 95% (pavement/sidewalks), detec. 80% (road marking)
[98]	Five 3D LiDAR sensors, and a multi-camera network	Curbs	ERFNet semantic segmentation, color projection of the semantic image pixel	Semantic labels analysis	Curb's lower and upper edge points searching, monotonically ascending region and vertical structure	precision 80% recall 60%
[99]	RIEGL VMX-450	Dashed line, text, straight arrow, turn arrow, diamond, triangle, lane line, and crossing	3D point clouds are first projected onto a horizontal plane and gridded as a 2D image	Segmentation network U-net to classify every pixel	A multiscale (distance-based Euclidean) clustering algorithm to large size road markings, and a CNN classifier to small size road markings	U-net-based Precision 95.97% Recall 87.52% F1-score 91.55%
[94]	RIEGL VMX-450	curb-based road surface extraction and multi threshold road marking extraction	Vehicle's trajectory data, MLS point clouds partition into a sequence of data blocks, corresponding profile sectioned with a certain width	Inverse distance weighting method, intensity and local-global elevation data, MLS road surface interpolation and Otsu for 2D intensity images	Sparse and unorganized road marking points clustered into topological and semantic objects using the conditional Euclidean clustering	recall 90.79%, precision 92.94%, and F1-score 91.85%
[95]	SSW	Manhole covers	Intensity-based images generation, fluctuation trend in the elevation to ground points extraction	HOG descriptor, PCA, symmetry characteristic, and shape detection, graph-based image segmentation method, OneCut	Dimension evaluation by sector decomposition diagram for manhole maintenance analysis	96.18%, complet. 94.27%, F-measure 95.22%
[89]	RIEGL VMX-450 AnnieWAY	Road boundary	The erroneous boundary removal is treated as a binary classification through a U-Net model	CNN-based method for 2D boundary completion, and Euclidean distance to partition the boundary points into separated line clusters	Matching taxi GPS trajectory points via boundary line images with centerline	91.34-92.14 complet. 89.87-95.91 correct. 82.81-88.65 quality
[103]	Five LiDAR and four monocular cameras	Vegetation, road, curb, lane marking, terrain and sidewalk	Semantically labeled images and projecting each LiDAR point onto the images	Extraction through semantic classes from region of consecutive points	Detection evaluation	avg distance 0.2-0.34 m prec. 63-84.2
[104]	Velodyne VLP-16	Road markings	Non road point filter based on the height difference	Road surface extraction by a moving fitting window filter from each pseudo-scan line	Marker edge detector with an intensity gradient and statistics histogram	Recall 90%, precision 95%, MCC 92%
[105]	Dataset1 Optech SG1 and Point Grey Dataset2 RIEGL VMX450	Road markings	Non-ground filtering and section alignment	A number of candidate are detected using HT algorithm	Fuzzy inference system	Avarage 88% F1-score and 87%

4.4. Road element detection and classification

Table 6 lists relevant works dealing with or proposing methods for road element detection and classification. Wen *et al.* [89] obtained critical information on urban roads ensures traffic safety. Road elements comprise curbs, lines, and road markings, among others. Road inventory is essential for adequate transportation management, advanced driver-assistance systems (ADAS), road network maintenance, traffic analysis, and traffic inspection. The first step in road element detection is conducting ground point filtering . Height filters can help extract the rest of the urban objects. Works searching for curbs and sidewalks start with a vertically 2D projection of point clouds. Then, they use intensity and height data to identify the elements. On the other hand, the task of searching for lines, arrows, pedestrian crossings, and dashed lines begins by conducting a horizontally 2D projection of segmented ground point clouds. Intensity values also help detect these elements. Researchers in [90], [91] use k-means and intensity filters jointly for detecting road elements. The first work detects pedestrian crossing and arrows using geometry based feature (GBF) extraction and classification. In the second work, sidewalk and pavement were identified by segmenting points whose normal vectors were close to the z-axis. 2D image generation helps identify urban elements of interest by 2D image methods. 2D image representation of road marking looks like gray or binary images. Researchers [34], [25] relied on the morphological method to process the information and detect road markings. Similarly, in [92]-[94], researchers applied the Otsu thresholding method to extract urban elements of interest. Other 2D image detection methods include Harris corner detector [35], principal component analysis (PCA) [93], HOG [95], and GBF extraction and classification [51], [90]. As reported in the literature, many methods can be used to assess detection accuracy, including Markov chain Monte Carlo (MCMC) methods, the Bayesian paradigm [96], [97], and CNNs [98], [99].

5. DISCUSSION

This review discusses the general applications of MLS systems merge with vision systems in urban management tasks. According to the review and Figure 2, RIEGL VMX-450, Optech Lynx Mobile Mapper, and Velodyne HDL-64 are the most popular MLS tools for managing urban tasks. RIEGL VMX-450 is a robust integrated system with its own sensors; Optech Lynx Mobile Mapper, however, is less robust than RIEGL but includes both digital cameras and GPS receivers. In turn, the Velodyne HDL-64 laser scanner sensor is robust but only comprises a laser scanner sensor. In conclusion, the choice of a given MLS system over the others may largely depend on multiple factors, such as costs. Integrated MLS systems are more appropriate since while the cameras can capture photogrammetric information then LiDAR can extract geometrical data, and GPSs retrieve object global location. Most of the works dealing with or proposing alternatives for urban object classification share the following standardized methodological structure: i) They perform geo-referenced point cloud and imagery data acquisition; ii) The data on the ground, facades, and the remaining objects are processed (i.e. data processing); iii) They propose a specific segmentation and detection method for the particular problem to be solved, and iv) Finally, they propose a classification method and assess the accuracy of the classified results.

Tendency in Figure 3 shows that 3D point cloud and imagery detection and classification problems regarding urban objects are growing at their own step. They apparently remain constant as we can see in the Figure 3. The mixed dynamic and static urban objects and mixed static urban objects works number are almost the same year by year. In contrasts, since approximately 2015 works about road sign and road elements detection and classification are increasing.

Contemporary initiatives to accomplish urban tasks are searching for specific goals with new proposals. For instance, buildings detection and reconstruction intend to retrieve occlusion and texture. Hyperspectral cameras are useful in tree, building energy, and pedestrian detection. Traffic elements are labeled using high retro-reflective paint for easy identification at night. Likewise, road elements are detected and discerned among them by intensity values (e.g. sidewalks, curves, lines, pedestrian crossings). The literature also discusses the detection and classification of retro-reflective and non-retro-reflective elements. Finally, 3D point cloud and 2D texture projection allows experts to apply well-known image processing methods.

In the use of MLS systems and vision systems, a disadvantage persists concerning to manual and offline algorithms training. Algorithms are hard run in real-time, and a part of the object detection and classification process is performed manually or offline. Thus, the training work depends on human experience and knowledge, and algorithm robustness bets on different lighting conditions, shadows, and urban landscape. It also seems that when searching for two or more urban object classes, avoiding extracting greater details

improves accuracy. Works detecting different objects hardly extract greater details. In this sense, semantic features seem to contribute to the solution, since they serve as the basic conceptual description of meaning for any element and contribute to having large labeled data sets.

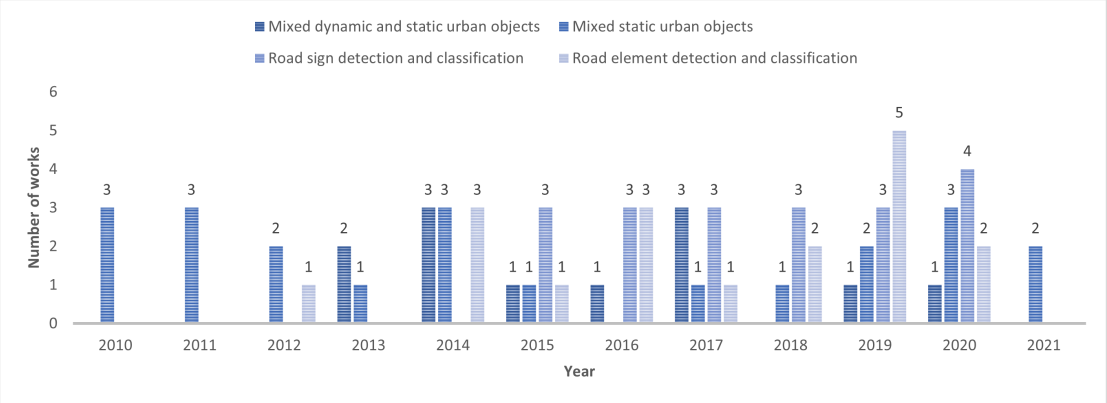

Figure 3. Tendency in our tables organization per year: i) mixed dynamic and static urban objects, ii) mixed static urban objects, iii) road sign detection and classification, and iv) road element detection and classification

6. SUGGESTED FUTURE RESEARCH

MLS systems that integrate GPS receivers and cameras grant simultaneous registration of visual and spatial data. Nevertheless, the high cost of these system features may imply that the current solution is a disadvantage. The developments explored in this review share some overall limitations and challenges. Two of the most common problems are the existence of large occluded regions and segmentation. Different authors propose learning and searching for occluded parts. They suggest that several scan images of the same area could mitigate this problem; however, segmentation methods are by themselves a case of study. Another critical issues are the under-segmentation and over-segmentation of point clouds. The improvement of segmentation processes have to include an analysis of object density, shape, color, and texture; some promising works add intensity gradient, spectral features, and geometric features. We also found that the gray-scale and binary information are the most used features for object segmentation, followed by the RGB color space; however, other color spaces such as HSV or CMYK can improve the segmentation and classification of different objects by relying on a broader range of color shades. MMS including LiDAR and cameras are applied to other urban tasks and can consequently benefit a range of industries and disciplines. This review provided an overview of the multiple industries benefitting from MMS developments for particular application: i) Automotive industries: vehicle statistics analysis, accident statistics analysis, electronic unit development for road assistance and vehicle driving; ii) Urban planning and 3D reconstruction: road dimensions and directions, identification of sidewalk characteristics, building classification, bus stop detection, light detection, ramp detection, pedestrian crossing detection, and road sign identification. Management of transportation, commerce, recreational, and environmental projects, and study of touristic places; iii) Construction industries: drainage system management, complementary works, signaling dynamics, weather forecast, and obstacle detection for road sign installation; iv) Data collection companies: socio-demographic data collection, trade applications, construction, employment home and housing projects, map development, environmental studies, population, transport, and tourism; and v) Telecommunication and other digital technology companies: utility pole detection, street name sign detection, road sign detection, identification of regional borders, railroad detection, green area data collection, and socioeconomic data collection.

New urban management developments must contemplate as sources of data government databases in order to meet their goals. Finally, some of the reviewed works discuss the feasibility of a further fusion of their systems with complementary sensors, such as radars, video cameras, and encoders, to name a few.

7. CONCLUSION

This review discussed the use of 3D point cloud data with imagery in urban management applications. The goal of the review was to highlight the MMS and MLS systems currently available for handling urban management tasks. Additionally, our review discussed current trends in urban object segmentation, detection, and classification. We considered urban management applications such as historic preservation, roadside assistance, road infrastructure inventory, and public space study. Urban element detection aims at maintaining order between dynamic and static variables. Dynamic object detection (e.g. pedestrians and cars) is mostly conducted for self-driving assistance, driver assistance, and traffic scene analysis. On the other hand, detection of road markings and road signs contribute to successful traffic inspection, road system maintenance, and driver safety. Urban elements are key guidance assets within the road system; hence, pedestrians and drivers have to be easily detectable. Recurrent inspections of road elements guarantee their visibility, maintenance, and ability to provide the necessary road information. Unfortunately, the costs of road infrastructure maintenance increase as roads deteriorate. From this perspective, MLS systems promise to be a feasible solution to prevent serious road deterioration through constant monitoring, even though it is necessary to prove the advantages of both automatic and manual acquisition inspections. The latest works on road sign detection revolved around using D-ANNs, implying that this path might be the best for urban element identification. Even though the results are favorable, there is still some uncertainty surrounding the use of such a powerful tool for a small problem. Choosing deep learning and classical methods of machine learning depends on several factors, such as the amount of data to be identified. For some urban elements, their identification is sometimes troublesome, even with well-known and well-defined variables occluded, altered, or damaged. In this case, it is advised to consider both D-ANNs and machine learning options.

ACKNOWLEDGEMENT

CONACYT México and IPN México for the Ph.D student grant 584190. Financial support given by SIP-IPN (20210280 and 20201942). The primary sponsor of this research is the National Consortium of Scientific and Technological Information Resources (CONRICYT, for its Spanish acronym) of Mexico.

REFERENCES

[1] Y. Lin and J. Hyyppa, "Geometrically modeling 2d scattered points: a review of the potential for methodologically improving mobile laser scanning in data processing," *International Journal of Digital Earth*, vol. 7, no. 6, pp. 432–449, 2014, doi: 10.1080/17538947.2013.781239.

[2] L. Cheng, S. Chen, X. Liu, H. Xu, Y. Wu, M. Li, and Y. Chen, "Registration of laser scanning point clouds: A review," *Sensors*, vol. 18, no. 5, 2018, doi: 10.3390/s18051641.

[3] I. Puente, H. Gonzalez-Jorge, P. Arias, and J. Armesto, "Land-based mobile laser scanning systems: A review," in *ISPRS - International Archives of the Photogrammetry Remote Sensing and Spatial Information Sciences XXXVIII-5/W12*, 2011, vol. XXXVIII-5/W12, pp. 163–168, doi: 10.5194/isprsarchives-XXXVIII-5-W12-163-2011.

[4] I. Jazayeri, A. Rajabifard, and M. Kalantari, "A geometric and semantic evaluation of 3d data sourcing methods for land and property information," *Land Use Policy*, vol. 36, pp. 219–230, 2014, doi: 10.1016/j.landusepol.2013.08.004.

[5] R. Lindenbergh and P. Pietrzyk, "Change detection and deformation analysis using static and mobile laser scanning," *Applied Geomatics*, vol. 7, no. 2, p. 65–74, 2015, doi: 10.1007/s12518-014-0151-y.

[6] W. Mukupa, G. W. Roberts, C. M. Hancock, and K. Al-Manasir, "A review of the use of terrestrial laser scanning application for change detection and deformation monitoring of structures," *Survey Review*, vol. 49, no. 353, pp. 99–116, 2017, doi: 10.1080/00396265.2015.1133039.

[7] L. Matikainen, M. LehtomA¤ki, E. Ahokas, J. Hyyppa, M. Karjalainen, A. Jaakkola, A. Kukko, and T. Heinonen, "Remote sensing methods for power line corridor surveys," *ISPRS Journal of Photogrammetry and Remote Sensing*, vol. 119, pp. 10 – 31, 2016, doi: 10.1016/j.isprsjprs.2016.04.011.

[8] E. Che, J. Jung, and M. J. Olsen, "Object recognition, segmentation, and classification of mobile laser scanning point clouds: A state of the art review," *Sensors*, vol. 19, no. 4, pp. 810, 2019, doi: 10.3390/s19040810.

[9] Y. Wang, Q. Chen, Q. Zhu, L. Liu, C. Li, and D. Zheng, "A survey of mobile laser scanning applications and key techniques over urban areas," *Remote Sensing*, vol. 11, no. 13, 2019, doi: 10.3390/rs11131540.

[10] C. Wang, C. Wen, Y. Dai, S. Yu, and M. Liu, "Urban 3d modeling with mobile laser scanning: a review," *Virtual Reality & Intelligent Hardware*, vol. 2, no. 3, pp. 175 – 212, 2020, doi: 10.1016/j.vrih.2020.05.003.

[11] R. Wang, "3d building modeling using images and lidar: a review," *International Journal of Image and Data Fusion*, vol. 4, no. 4 pp. 273 – 292, 2013, doi: 10.1080/19479832.2013.811124.

[12] P. Musialski, P. Wonka, D. G. Aliaga, M. Wimmer, L. van Gool, and W. Purgathofer, "A survey of urban reconstruction," *Computer Graphics Forum*, vol. 32, no. 6, pp. 146–177, 2013, doi: 10.1111/cgf.12077.

[13] I. Puente, H. Gonzalez-Jorge, J. Martınez-Sanchez, and P. Arias, "Review of mobile mapping and surveying technologies," *Measurement*, vol. 46, no. 7, pp. 2127–2145, 2013, doi: 10.1016/j.measurement.2013.03.006.

[14] H. Guan, J. Li, S. Cao, and Y. Yu, "Use of mobile lidar in road information inventory: a review," *International Journal of Image and Data Fusion*, vol. 7, no. 3, pp. 219–242, 2016, doi: 10.1080/19479832.2016.1188860.
[15] L. Ma, Y. Li, J. Li, C. Wang, R. Wang, and M. A. Chapman, "Mobile laser scanned point-clouds for road object detection and extraction: A review," *Remote Sensing*, vol. 10, no. 10, pp. 1531, 2018, doi: 10.3390/rs10101531.
[16] M. Soilan, A. Sanchez-Rodriguez, P. del Rio-Barral, C. Perez-Collazo, P. Arias, and B. Riveiro, "Review of laser scanning technologies and their applications for road and railway infrastructure monitoring," *Infrastructures*, vol. 4, no. 4, pp. 58, 2019, doi: 10.3390/infrastructures4040058.
[17] C. Wang, C. Wen, Y. Dai, S. Yu, and M. Liu, "Urban 3d modeling with mobile laser scanning: a review," *Virtual Reality & Intelligent Hardware*, vol. 2, no. 3, pp. 175–212, 2020, doi: 10.1016/j.vrih.2020.05.003.
[18] B. Gao, Y. Pan, C. Li, S. Geng, and H. Zhao, "Are we hungry for 3d lidar data for semantic segmentation? a survey of datasets and methods," *IEEE Transactions on Intelligent Transportation Systems*, pp. 1–19, 2021, doi: 10.1109/TITS.2021.3076844.
[19] J. Zhang and X. Lin, "Advances in fusion of optical imagery and lidar point cloud applied to photogrammetry and remote sensing," International Journal of Image and Data Fusion, vol. 8, no. 1, pp. 1–31, 2016, doi: 10.1080/19479832.2016.1160960.
[20] H. Zhong, H. Wang, Z. Wu, C. Zhang, Y. Zheng, and T. Tang, "A survey of lidar and camera fusion enhancement," Procedia Computer Science, vol. 183, pp. 579–588, 2021, doi: 10.1016/j.procs.2021.02.100.
[21] A. Jaakkola, J. Hyyppa, A. Kukko, X. Yu, H. Kaartinen, M. Lehtom ¨ aki, and Y. Lin, "A low-cost multi-sensoral mobile mapping system and its feasibility for tree measurements," *ISPRS Journal of Photogrammetry and Remote Sensing*, vol. 65, no. 6, pp. 514–522, 2010, doi: 10.1016/j.isprsjprs.2010.08.002.
[22] E. Puttonen, A. Jaakkola, P. Litkey, and J. Hyyppa, "Tree classification with fused mobile laser scanning and hyperspectral data," *Sensors*, vol. 11, no. 5, pp. 5158–5182, 2011, doi: 10.3390/s110505158.
[23] L. Smadja, J. Ninot, and T. Gavrilovic, "Road extraction and environment interpretation from LIDAR sensors," In: N. Paparoditis, M. Pierrot-Deseilligny, C. Mallet, and O. Tournaire (Eds), *IAPRS*, vol. 38, 2010.
[24] P. Kumar, T. Mccarthy, and C. Mc Elhinney, "Automated road extraction from terrestrial based mobile laser scanning system using the gvf snake model," in *European LiDAR Mapping Forum (ELMF 2010)*, 2010, pp. 1–11. [Online]. Available: http://mural.maynoothuniversity.ie/12794.
[25] P. Kumar, C. Mc Elhinney, P. Lewis, and T. Mccarthy, "Automated road markings extraction from mobile laser scanning data," *International Journal of Applied Earth Observation and Geoinformation*, vol. 32, pp. 125–137, 2014, doi: 10.1016/j.jag.2014.03.023.
[26] Y. Hu, X. Li, J. Xie, and L. Guo, "A novel approach to extracting street lamps from vehicle-borne laser data," in *Proceedings - 2011 19th International Conference on Geoinformatics, Geoinformatics 2011*, 2011, pp. 1–6, doi: https: 10.1109/GeoInformatics.2011.5981183.
[27] D. M. Chen *et al.*, "City-scale landmark identification on mobile devices," *CVPR 2011*, 2011, pp. 737-744, doi: 10.1109/CVPR.2011.5995610.
[28] P. Babahajiani, L. Fan, and M. Gabbouj, "Semantic Parsing of Street Scene Images Using 3D LiDAR Point Cloud," *2013 IEEE International Conference on Computer Vision Workshops*, 2013, pp. 714-721, doi: 10.1109/ICCVW.2013.98.
[29] A.-I. Garc´ıa-Moreno, J.-J. Gonzalez-Barbosa, F.-J. Ornelas-Rodriguez, H.-R. Juan-Bautista, A. Ramirez-Pedraza, and E.-A. Gonzalez-Barbosa, "Automatic 3d city reconstruction platform using a lidar and dgps," in *Advances in Artificial Intelligence*, 2012, doi: 10.1007/978-3-642-37807-2 25.
[30] A.-I. Garcia-Moreno, J.-J. Gonzalez-Barbosa, A. Ramirez-Pedraza, J. B. Hurtado-Ramos, and F.-J. Ornelas-Rodriguez, "Complete Sensitivity Analysis in a LiDAR-Camera Calibration Model," *Journal of Computing and Information Science in Engineering*, vol. 16, no. 1, 2015, p. 014501, doi: 10.1115/1.4032026.
[31] A. I. Garc´ıa Moreno and J.-J. Gonzalez-Barbosa, "Virtual 3d reconstruction of complex urbanenvironments," *Revista Iberoamericana de Automatica e Informatica industrial* , vol. 17, pp. 22, 2020. [Online]. Available: https://polipapers.upv.es/index.php/RIAI/article/view/11203
[32] K. Gajdamowicz, D. Ohman, and M. Horemu ¨ z, "Mapping and 3d modelling of urban ˇ environment based on lidar, gps/imu and image data," *ISPRS*, 2012, doi: 10.1.1.222.5218
[33] N. Paparoditis, J.-P. Papelard, B. Cannelle, A. Devaux, B. Soheilian, N. David, and E. Houzay, "Stereopolis ii: A multi-purpose and multi-sensor 3d mobile mapping system for street visualisation and 3d metrology," *Revue Franaise de Photogrammetrie et de Teledetection*, vol. 200, pp. 69–79, 2012, doi: 10.52638/rfpt.2012.63.
[34] A. Mancini, E. Frontoni, and P. Zingaretti, "Automatic road object extraction from mobile mapping systems," in *Proceedings of 2012 IEEE/ASME 8th IEEE/ASME International Conference on Mechatronic and Embedded Systems and Applications*, July 2012, pp. 281–286, doi: 10.1109/MESA.2012.6275575.
[35] Z. Hussnain, S. Oude Elberink, and G. Vosselman, "Automatic feature detection, description and matching from mobile laser scanning data and aerial imagery," *ISPRS - International Archives of the Photogrammetry, Remote Sensing and Spatial Information Sciences*, vol. XLI-B1, pp. 609–616, 2016, doi: 10.5194/isprs-archives-XLI-B1-609-2016.
[36] I. Puente, H. Gonzalez-Jorge, J. Martınez-Sanchez, and P. Arias, "Automatic detection of road tunnel luminaires using a mobile lidar system," *Measurement*, vol. 47, pp. 569 – 575, 2014, doi: 10.1016/j.measurement.2013.09.044.
[37] B. Riveiro, L. D´ıaz Vilarino, B. Conde, M. Soilan, and P. Arias, "Automatic segmentation and shape-based classification of retro-reflective traffic signs from mobile lidar data," *IEEE Journal of Selected Topics in Applied Earth Observations and Remote Sensing*, vol. 9, pp. 1–9, 2015, doi: 10.1109/JSTARS.2015.2461680.
[38] M. Soilan, B. Riveiro, J. Martınez-Sanchez, and P. Arias, "Traffic sign detection in mls acquired point clouds for geometric and image-based semantic inventory," *ISPRS Journal of Photogrammetry and Remote Sensing*, vol. 114, pp. 92–101, 2016, doi: 10.1016/J.ISPRSJPRS.2016.01.019.
[39] A. Arcos-Garcia, M. Soilan, J. Alvarez-Garcia, and B. Riveiro, "Exploiting syner- ´ gies of mobile mapping sensors and deep learning for traffic sign recognition systems," *Expert Systems with Applications*, vol. 89, 2017, doi: 10.1016/j.eswa.2017.07.042
[40] A. H. Safaie, H. Rastiveis, A. Shams, W. A. Sarasua, and J. Li, "Automated street tree inventory using mobile lidar point clouds based on hough transform and active contours," *ISPRS Journal of Photogrammetry and Remote Sensing*, vol. 174, pp. 19–34, 2021, doi: 10.1016/j.isprsjprs.2021.01.026.
[41] R. Zhong, J. Wei, W. Su, and Y. F. Chen, "A method for extracting trees from vehicle-borne laser scanning data," *Mathematical and*

Computer Modelling, vol. 58, no. 3, pp. 733–742, 2013, doi: 10.1016/j.mcm.2012.12.038.
[42] B. Yang, Z. Dong, G. Zhao, and W. Dai, "Hierarchical extraction of urban objects from mobile laser scanning data," *ISPRS Journal of Photogrammetry and Remote Sensing*, vol. 99, pp. 45–57, 2014, doi: 10.1016/j.isprsjprs.2014.10.005.
[43] J. Landa and D. Prochazka, "Automatic road inventory using lidar," Procedia Economics and Finance, vol. 12, pp. 363–370, 2014, doi: 10.1016/S2212-5671(14)00356-6.
[44] S. Wu, C. Wen, H. Luo, Y. Chen, C. Wang, and J. Li, "Using mobile lidar point clouds for traffic sign detection and sign visibility estimation," in *2015 IEEE International Geoscience and Remote Sensing Symposium (IGARSS)*, July 2015, pp. 565–568, doi: 10.1109/IGARSS.2015.7325826.
[45] Y. Yu, J. Li, C. Wen, H. Guan, H. Luo, and C. Wang, "Bag-of-visual-phrases and hierarchical deep models for traffic sign detection and recognition in mobile laser scanning data," *ISPRS Journal of Photogrammetry and Remote Sensing*, vol. 113, pp. 106–123, 2016, doi: 10.1016/J.ISPRSJPRS.2016.01.005.
[46] C. Wen, J. Li, H. Luo, Y. Yu, Z. Cai, H. Wang, and C. Wang, "Spatial-related traffic sign inspection for inventory purposes using mobile laser scanning data," *IEEE Transactions on Intelligent Transportation Systems*, vol. 17, no. 1, pp. 27–37, Jan. 2016, doi: 10.1109/TITS.2015.2418214.
[47] C. You, C. Wen, H. Luo, C. Wang, and J. Li, "Rapid traffic sign damage inspection in natural scenes using mobile laser scanning data," in *2017 IEEE International Geoscience and Remote Sensing Symposium (IGARSS)*, July 2017, pp. 6271–6274, doi: 10.1109/IGARSS.2017.8128440.
[48] H. Guan, W. Yan, Y. Yu, L. Zhong, and D. Li, "Robust traffic-sign detection and classification using mobile lidar data with digital images," *IEEE Journal of Selected Topics in Applied Earth Observations and Remote Sensing*, vol. 11, no. 5, pp. 1715–1724, May 2018, doi: 10.1109/JSTARS.2018.2810143.
[49] H. Guan, Y. Yu, D. Li, and J. Li, "Automatic traffic sign detection and recognition using mobile lidar data with digital images," *ISPRS - International Archives of the Photogrammetry, Remote Sensing and Spatial Information Sciences*, vol. XLIII-B3-2020, pp. 599–603, 2020, doi: 10.5194/isprs-archives-XLIII-B3-2020-599-2020.
[50] H. Guan, J. Li, Y. Yu, and Y. Liu, "Geometric validation of a mobile laser scanning system for urban applications," in *2015 ISPRS International Conference on Computer Vision in Remote Sensing*, 2016, p. 990108, doi: 10.1117/12.2234907.
[51] N. Sairam, S. Nagarajan, and S. Ornitz, "Development of mobile mapping system for 3d road asset inventory," *Sensors*, vol. 16, pp. 367, 2016, doi: 10.3390/s16030367.
[52] R. Ravi, Y. Lin, M. Elbahnasawy, T. Shamseldin, and A. Habib, "Simultaneous system calibration of a multi-lidar multicamera mobile mapping platform," *IEEE Journal of Selected Topics in Applied Earth Observations and Remote Sensing*, vol. 11, no. 5, pp. 1694–1714, May 2018, doi: 10.1109/JSTARS.2018.2812796.
[53] M. Khalilikhah, K. Heaslip, and K. Hancock, "Traffic sign vandalism and demographics of local population: A case study in utah," *Journal of Traffic and Transportation Engineering (English Edition)*, vol. 3, no. 3, pp. 192 – 202, 2016, doi: 10.1016/j.jtte.2015.11.001.
[54] M. Khalilikhah, G. Fu, K. Heaslip, and P. Carlson, "Analysis of in-service traffic sign visual condition: Tree-based model for mobile lidar and digital photolog data," *Journal of Transportation Engineering Part A: Systems*, vol. 144, p. 04018017, 2018, doi: 10.1061/JTEPBS.0000132.
[55] T. Cui, S. Ji, J. Shan, J. Gong, and K. Liu, "Line-based registration of panoramic images and lidar point clouds for mobile mapping," *Sensors*, vol. 17, no. 1, 2017, doi: 10.3390/s17010070.
[56] M. Yadav and C. G. Chousalkar, "Extraction of power lines using mobile lidar data of roadway environment," *Remote Sensing Applications: Society and Environment*, vol. 8, pp. 258–265, 2017, doi: 10.1016/j.rsase.2017.10.007.
[57] M. Yadav, B. Lohani, and A. K. Singh, "Road surface detection from mobile lidar data," *ISPRS Annals of the Photogrammetry*, Remote Sensing and Spatial Information Sciences, vol. 45, pp. 95–101, 2018, doi: 10.5194/ISPRS-ANNALS-IV-5-95-2018.
[58] M. Yadav, A. K. Singh, and B. Lohani, "Computation of road geometry parameters using mobile lidar system," *Remote Sensing Applications: Society and Environment*, vol. 10, pp. 18–23, 2018, doi: 10.1016/j.rsase.2018.02.003.
[59] Z. Deng and L. Zhou, "Detection and recognition of traffic planar objects using colorized laser scan and perspective distortion rectification," *IEEE Transactions on Intelligent Transportation Systems*, vol. 19, no. 5, pp. 1485-1495, 2018, doi: 10.1109/TITS.2017.2723902.
[60] B. Borgmann, V. Schatz, H. Kieritz, C. Scherer-Klockling, M. Hebel, and M. Arens, "Data processing and recording using a versatile multi-sensor vehicle," *ISPRS Annals of the Photogrammetry, Remote Sensing and Spatial Information Sciences* , vol. IV-1, pp. 21–28, 2018, doi: 10.5194/isprs-annals-IV-1-21-2018.
[61] D. R. Bruno, D. O. Sales, J. Amaro, and F. S. Osório, "Analysis and fusion of 2D and 3D images applied for detection and recognition of traffic signs using a new method of features extraction in conjunction with Deep Learning," *2018 International Joint Conference on Neural Networks (IJCNN)*, 2018, pp. 1-8, doi: 10.1109/IJCNN.2018.8489538.
[62] A. Buyval, A. Gabdullin, and M. Lyubimov, "Road sign detection and localization based on camera and lidar data," in *Eleventh International Conference on Machine Vision (ICMV 2018)*, 2019, vol. 11041, p. 1104125, doi: 10.1117/12.2523155.
[63] J. Jeong, Y. Cho, Y.-S. Shin, H. Roh, and A. Kim, "Complex urban dataset with multi-level sensors from highly diverse urban environments," *The International Journal of Robotics Research*, vol. 38, no. 6, pp. 642–657, 2019, doi: 10.1177/0278364919843996.
[64] W. Tan, N. Qin, L. Ma, Y. Li, J. Du, G. Cai, K. Yang, and J. Li, "Toronto-3d: A large-scale mobile lidar dataset for semantic segmentation of urban roadways," in *2020 IEEE/CVF Conference on Computer Vision and Pattern Recognition, CVPR Workshops 2020*, 2020, pp. 797–806, doi: 10.1109/CVPRW50498.2020.00109.
[65] J. Zhu, Y. Xu, Z. Ye, L. Hoegner, and U. Stilla, "Fusion of urban 3d point clouds with thermal attributes using mls data and tir image sequences," *Infrared Physics & Technology*, vol. 113, p. 103622, 2021, doi: 10.1016/j.infrared.2020.103622.
[66] G. Zhao, X. Xiao, J. Yuan, and G. W. Ng, "Fusion of 3d-lidar and camera data for scene parsing," *Journal of Visual Communication and Image Representation*, vol. 25, no. 1, pp. 165–183, 2014, doi: 10.1016/j.jvcir.2013.06.008.
[67] P. Babahajiani, L. Fan, J. -K. Kämäräinen, and M. Gabbouj, "Comprehensive automated 3D urban environment modelling using terrestrial laser scanning point cloud," *2016 IEEE Conference on Computer Vision and Pattern Recognition Workshops (CVPRW)*, 2016, pp. 652-660, doi: 10.1109/CVPRW.2016.87.
[68] P. Babahajiani, L. Fan, J.-K. Kämäräinen, and M. Gabbouj, "Urban 3d segmentation and modelling from street view images and

lidar point clouds," *Machine Vision and Applications*, vol. 28, pp. 679–694, 2017, doi: 10.1007/s00138-017-0845-3.
[69] J. Balado, R. Sousa, L. Diaz-Vilarino, and P. Arias, "Transfer learning in urban object classification: Online images to recognize point clouds," *Automation in Construction*, vol. 111, p. 103058, 2020, doi: 10.1016/j.autcon.2019.103058.
[70] B. Soheilian, O. Tournaire, N. Paparoditis, B. Vallet, and J. Papelard, "Generation of an integrated 3D city model with visual landmarks for autonomous navigation in dense urban areas," *2013 IEEE Intelligent Vehicles Symposium (IV)*, 2013, pp. 304-309, doi: 10.1109/IVS.2013.6629486.
[71] M. Lehtomäki *et al.*, "Object Classification and Recognition From Mobile Laser Scanning Point Clouds in a Road Environment," in *IEEE Transactions on Geoscience and Remote Sensing*, vol. 54, no. 2, pp. 1226-1239, Feb. 2016, doi: 10.1109/TGRS.2015.2476502.
[72] M. Soilan, B. Riveiro, A. Sanchez Rodriguez, and P. Arias, "Safety assessment on pedestrian crossing environments using mls data," *Accident; analysis and prevention*, vol. 111, pp. 328–337, 2017, doi: 10.1016/j.aap.2017.12.009.
[73] Z. Luo, J. Li, Z. Xiao, Z. G. Mou, X. Cai, and C. Wang, "Learning high-level features by fusing multi-view representation of mls point clouds for 3d object recognition in road environments," *ISPRS Journal of Photogrammetry and Remote Sensing*, vol. 150, pp. 44–58, 2019, doi: 10.1016/j.isprsjprs.2019.01.024.
[74] A. Serna and B. Marcotegui, "Detection, segmentation and classification of 3d urban objects using mathematical morphology and supervised learning," *ISPRS Journal of Photogrammetry and Remote Sensing*, vol. 93, pp. 243–255, 2014, doi: 10.1016/j.isprsjprs.2014.03.015.
[75] A. Börcs, B. Nagy, and C. Benedek, "Instant object detection in Lidar point clouds," in *IEEE Geoscience and Remote Sensing Letters*, vol. 14, no. 7, pp. 992-996, July 2017, doi: 10.1109/LGRS.2017.2674799.
[76] R. Qin and A. Gruen, "3d change detection at street level using mobile laser scanning point clouds and terrestrial images," *ISPRS Journal of Photogrammetry and Remote Sensing*, vol. 90, pp. 23–35, 2014, doi: 10.1016/J.ISPRSJPRS.2014.01.006.
[77] J.-H. Im, S.-H. Im, and G.-I. Jee, "Extended line map-based precise vehicle localization using 3d lidar," *Sensors*, vol. 18, no. 10, 2018, doi: 10.3390/s18103179.
[78] B. Yang, Z. Wei, Q. Li, and J. Li, "Automated extraction of street-scene objects from mobile lidar point clouds," *International Journal of Remote Sensing*, vol. 33, no. 18, pp. 5839–5861, 2012, doi: 10.1080/01431161.2012.674229.
[79] S. Van Ackere, J. Verbeurgt, L. De Sloover, A. Wulf, N. Van de Weghe, and P. De Maeyer, "Extracting dimensions and locations of doors, windows, and door thresholds out of mobile lidar data using object detection to estimate the impact of floods," *International Archives of the Photogrammetry, Remote Sensing and Spatial Information Sciences*, vol. XLII-3/W8, pp. 429–436, 2019, doi: 10.5194/isprs-archives-XLII-3-W8-429-2019.
[80] B. Ergun, C. Sahin, and A. Aydin, "Two-dimensional (2-d) kalman segmentation approach in mobile laser scanning (mls) data for panoramic image registration," *Lasers in Engineering*, vol. 48, pp. 121–150, 2020. [Online]. Available: https://www.oldcitypublishing.com/journals/lie-home/lie-issuecontents/lie-volume-48-number-1-3-2021/lie-48-1-3-p-121-150/.
[81] G. Uggla and M. Horemuz, "Identifying roadside objects in mobile laser scanning data using image-based point cloud segmentation," *Journal of Information Technology in Construction*, vol. 25, pp. 545–560, 2020, doi: 10.36680/j.itcon.2020.031.
[82] W. Liu *et al.*, "Learning to match 2D images and 3D LiDAR point clouds for outdoor augmented reality,"*2020 IEEE Conference on Virtual Reality and 3D User Interfaces Abstracts and Workshops (VRW)*, 2020, pp. 654-655, doi: 10.1109/VRW50115.2020.00178.
[83] H. Guan, Y. Yu, Z. Ji, J. Li, and Q. Zhang, "Deep learning-based tree classification using mobile lidar data," *Remote Sensing Letters*, vol. 6, no. 11, pp. 864–873, 2015, doi: 10.1080/2150704X.2015.1088668.
[84] X. Gong, D. Wei and G. Zhou, "Extracting trees and structure parameters via integration of LIDAR data and ground imagery," *2010 IEEE International Geoscience and Remote Sensing Symposium*, 2010, pp. 2703-2706, doi: 10.1109/IGARSS.2010.5650078.
[85] K. Flores-Rodriguez, J. Gonzlez-Barbosa, F. Ornelas-Rodriguez, J. Hurtado-Ramos, and P. Ramirez-Pedraza, "Road signs segmentation through mobile laser scanner and imagery," *Advances in Computational Intelligence, MICAI 2020. Lecture Notes in Computer Science*, Martínez-Villaseñor L., Herrera-Alcántara O., Ponce H., Castro-Espinoza F.A. (Eds), vol. 12469, 2020, doi: 10.1007/978-3-030-60887-3_33.
[86] C. You, C. Wen, C. Wang, J. Li, and A. Habib, "Joint 2-D–3-D traffic sign landmark data set for geo-localization using mobile laser scanning data," in *IEEE Transactions on Intelligent Transportation Systems*, vol. 20, no. 7, pp. 2550-2565, July 2019, doi: 10.1109/TITS.2018.2868168.
[87] H. Guan *et al.*, "A convolutional capsule network for traffic-sign recognition using mobile LiDAR data with digital images," *in IEEE Geoscience and Remote Sensing Letters*, vol. 17, no. 6, pp. 1067-1071, June 2020, doi: 10.1109/LGRS.2019.2939354.
[88] H. Guan, Y. Yu, D. Li, and J. Li, "Automatic traffic sign detection and recognition using mobile lidar data with digital images," *ISPRS - International Archives of the Photogrammetry, Remote Sensing and Spatial Information Sciences*, vol. XLIII-B3-2020, pp. 599–603, 2020, doi: 10.5194/isprs-archives-XLIII-B3-2020-599-2020.
[89] C. Wen, C. You, H. Wu, C. Wang, X. Fan, and J. Li, "Recovery of urban 3d road boundary via multi-source data," *ISPRS Journal of Photogrammetry and Remote Sensing*, vol. 156, pp. 184 – 201, 2019, doi: 10.1016/j.isprsjprs.2019.08.010.
[90] M. Soilan, B. Riveiro, J. Martinez-Sanchez, and P. Arias, "Segmentation and classification of road markings using mls data," *ISPRS Journal of Photogrammetry and Remote Sensing*, vol. 123, pp. 94–103, 2017, doi: 10.1016/j.isprsjprs.2016.11.011.
[91] M. Soilan, L. Truong-Hong, B. Riveiro, and D. Laefer, "Automatic extraction of road features in urban environments using dense als data," *International Journal of Applied Earth Observation and Geoinformation*, vol. 64, pp. 226 – 236, 2018, doi: [Online]. Available: https://core.ac.uk/download/pdf/162463945.pdf.
[92] H. Guan, J. Li, Y. Yu, C. Wang, M. Chapman, and B. Yang, "Using mobile laser scanning data for automated extraction of road markings," *ISPRS Journal of Photogrammetry and Remote Sensing*, vol. 87, pp. 93–107, 2014, doi: 10.1016/j.isprsjprs.2013.11.005.
[93] Y. Yu, J. Li, H. Guan, F. Jia, and C. Wang, "Learning hierarchical features for automated extraction of road markings from 3-d mobile lidar point clouds," *IEEE Journal of Selected Topics in Applied Earth Observations and Remote Sensing*, vol. 8, no. 2, pp. 709–726, Feb 2015, doi: 10.1109/JSTARS.2014.2347276.
[94] L. Ma, Y. Li, J. Li, Z. Zhong, and M. A. Chapman, "Generation of horizontally curved driving lines in hd maps using mobile laser scanning point clouds," *IEEE Journal of Selected Topics in Applied Earth Observations and Remote Sensing*, vol. 12, no. 5, pp. 1572–1586, May 2019, doi: 10.1109/JSTARS.2019.2904514.
[95] Z. Wei, M. Yang, L. Wang, H. Ma, X. Chen, and R. Zhong, "Customized mobile lidar system for manhole cover detection and

identification," *Sensors*, vol. 19, no. 10, pp. 2422, 2019, doi: 10.3390/s19102422.
[96] Y. Yu, J. Li, H. Guan, C. Wang, and J. Yu, "Automated detection of road manhole and sewer well covers from mobile lidar point clouds," *IEEE Geoscience and Remote Sensing Letters*, vol. 11, pp. 1549–1553, Sept. 2014, doi: 10.1109/LGRS.2014.2301195.
[97] B. Soheilian, X. Qu, and M. Bredif, "Landmark based localization: Lba refinement using MCMC-optimized projections of RJMCMC-extracted road marks," in *2016 IEEE Intelligent Vehicles Symposium (IV)*, June 2016, pp. 940–947, doi: 10.1109/IVS.2016.7535501.
[98] S. E. C. Goga and S. Nedevschi, "Fusing semantic labeled camera images and 3d lidar data for the detection of urban curbs," in *2018 IEEE 14th International Conference on Intelligent Computer Communication and Processing (ICCP)*, Sep. 2018, pp. 301–308, doi: 10.1109/ICCP.2018.8516649.
[99] C. Wen, X. Sun, J. Li, C. Wang, Y. Guo, and A. Habib, "A deep learning framework for road marking extraction, classification and completion from mobile laser scanning point clouds," *ISPRS Journal of Photogrammetry and Remote Sensing*, vol. 147, pp. 178 – 192, 2019, doi: 10.1016/j.isprsjprs.2018.10.007.
[100] A. Novo, H. Gonzalez-Jorge, J. Martinez-Sanchez, and H. Lorenzo, "Canopy detection over roads using mobile lidar data," *International Journal of Remote Sensing*, vol. 41, no. 5, pp. 1927–1942, 2020, doi: 10.1080/01431161.2019.1678077.
[101] M. Khalilikhah, K. Heaslip, and Z. Song, "Can daytime digital imaging be used for traffic sign retroreflectivity compliance?," *Measurement*, vol. 75, pp. 147–160, 2015, doi: 10.1016/j.measurement.2015.07.049.
[102] S. Zhang, C. Wang, L. Lin, C. Wen, C. Yang, Z. Zhang, and J. Li, "Automated visual recognizability evaluation of traffic sign based on 3d lidar point clouds," *Remote Sensing*, vol. 11, no. 12, pp. 1453, 2019, doi: 10.3390/rs11121453.
[103] S. E. Catalina Deac, I. Giosan, and S. Nedevschi, "Curb detection in urban traffic scenarios using lidars point cloud and semantically segmented color images," in *2019 IEEE Intelligent Transportation Systems Conference (ITSC)*, 2019, pp. 3433–3440, doi: 10.1109/ITSC.2019.8917020.
[104] R. Yang, Q. Li, J. Tan, S. Li, and X. Chen, "Accurate road marking detection from noisy point clouds acquired by low-cost mobile lidar systems," *ISPRS International Journal of Geo-Information*, vol. 9, no. 10, pp. 608, 2020, doi: 10.3390/ijgi9100608.
[105] H. Rastiveis, A. Shams, W. A. Sarasua, and J. Li, "Automated extraction of lane markings from mobile lidar point clouds based on fuzzy inference," *ISPRS Journal of Photogrammetry and Remote Sensing*, vol. 160, pp. 149–166, 2020, doi: 10.1016/j.isprsjprs.2019.12.009.

BIOGRAPHIES OF AUTHORS

José-Joel González-Barbosa has two master degree, the first one was received in Electrical Engineering from the University of Guanajuato, Mexico in 1998, and the second one was received in Signal, Image and, Acoustics from National Polytechnic Institute of Toulouse, France in 2000. He received his PhD. degree in Computer Science and Telecommunications from National Polytechnic Institute of Toulouse, France, in 2004. He is currently an Associate Professor at the CICATA-IPN, Mexico, where he teaches courses in computer vision, image processing, pattern recognition and scientific computing. His research interests include multicamera systems, 3D computer vision, panoramic vision, object recognition, robotics, augmented and virtual reality. He is affiliated with IEEE member. He can be contacted at email: jgonzalezba@ipn.mx.

Karen Lizbeth Flores-Rodríguez Her professional training includes a Bachelor's Degree in Mechatronics from the Polytechnic University of Sinaloa in 2012. She completed a master's degree in Robotics at the Technological University of Mixteca, Oaxaca, in 2017. She is currently a Ph.D. student in advanced technology, in the area of image analysis at CICATA-IPN Querétaro. Her areas of interest include computer vision, robotics, automation, artificial intelligence, and education. She can be contacted at email: kfloresr1800@alumno.ipn.mx.

Francisco Javier Ornelas-Rodríguez received his PhD. in Optics from the Research Center in Optics, México in 1999. His post-doc was spent at Computer Vision Center at Autonomous University of Barcelona (Spain) in 2002. Since 2007 is a Professor at Department of image analysis at Instituto Politecnico Nacional at CICATA Queretaro. Research interests, teaching experiences His fields of Researches are in Optical metrology applied to materials testing, image analysis applied in industry and 3D data object reconstruction. He was a researcher at CIATEC for 10 years at department of optoelectronics and was one of the initiators of the research area at CIATEC (1998-2007). He can be contacted at email: fornelasr@ipn.mx.

Felipe Trujillo-Romero received the Ph.D. degree in Informatics Systems from the Institut National Polytechnique de Toulouse France in 2008. At present, he is a full-time professor at the Department of Electronics Engineering, Universidad de Guanajuato. His research interests include computer vision, evolutionary algorithms, robotics, and parallel computing. He can be contacted at email: ftrujillo@mixteco.utm.mx.

Erick Alejandro González-Barbosa is a graduate research Mechanical Engineer from the University of Guanajuato, Mexico. He also completed his master's and doctorate degrees at the University of Guanajuato in 2006 and 2009. He is a research Professor at the Instituto Tecnológico Superior de Irapuato-ITESI, Mexico, teaches courses in dynamics, analysis and synthesis of mechanisms, mechanical design, and computer-aided design and engineering. His areas of interest include modeling and simulation of mechanical and mechatronic systems and kinematics and dynamics of industrial robots. He can be contacted at email: ergonzalez@itesi.edu.mx.

Juan B Hurtado-Ramos received the B.S. degree in Communications and Electronics Engineering in 1989 from the Guadalajara University. He obtained his Ph.D. degree from the Optics Research Center of the University of Guanajuato in 1999. He is currently a Professor-Researcher of the CICATA Querétaro-IPN, Mexico, in the Image Analysis group. His personal interests are mainly in the field of Metrology using optical techniques. Since 1998, he is a member of the Mexican National Researchers System. He can be contacted at email: jbautistah@ipn.mx.